ISSN 1854-6250

APEM *journal*

Advances in Production Engineering & Management

Volume 10 | Number 2 | June 2015

University of Maribor
Published by PEI
apem-journal.org

Advances in Production Engineering & Management

Identification Statement

ISSN 1854-6250 | Abbreviated key title: **Adv produc engineer manag** | Start year: 2006
ISSN 1855-6531 (on-line)

Published quarterly by **Production Engineering Institute (PEI)**, **University of Maribor**
Smetanova ulica 17, SI – 2000 Maribor, Slovenia, European Union (EU)

Phone: 00386 2 2207522, Fax: 00386 2 2207990
Language of text: English

APEM homepage: apem-journal.org
University homepage: www.um.si

APEM Editorial

Subscription Rate: 120 EUR for 4 issues (worldwide postage included); 30 EUR for single copies (plus 10 EUR for postage); for details about payment please contact: info@apem-journal.org

Postmaster: Send address changes to info@apem-journal.org

Cover and interior design by Miran Brezocnik
Printed by Tiskarna Koštomaj, Celje, Slovenia

APEM journal is indexed/abstracted in **Scopus** (Elsevier), **Inspec**, **EBSCO** (Academic Search Alumni Edition, Academic Search Complete, Academic Search Elite, Academic Search Premier, Engineering Source, Sales & Marketing Source, TOC Premier), **ProQuest** (CSA Engineering Research Database – Cambridge Scientific Abstracts, Materials Business File, Materials Research Database, Mechanical & Transportation Engineering Abstracts, ProQuest SciTech Collection), and **TEMA** (DOMA). Listed in **Ulrich's** Periodicals Directory and **Cabell's** Directory.

University of Maribor
Production Engineering Institute (PEI)

Advances in Production Engineering & Management

Volume 10 | Number 2 | June 2015 | pp 55–110

Contents

Journal homepage: apem-journal.org

ISSN 1854-6250
ISSN 1855-6531 (on-line)

Scope and topics

Advances in Production Engineering & Management (*APEM journal*) is an interdisciplinary refereed international academic journal published quarterly by the *Production Engineering Institute* at the *University of Maribor*. The main goal of the *APEM journal* is to present original, high quality, theoretical and application-oriented research developments in all areas of production engineering and production management to a broad audience of academics and practitioners. In order to bridge the gap between theory and practice, applications based on advanced theory and case studies are particularly welcome. For theoretical papers, their originality and research contributions are the main factors in the evaluation process. General approaches, formalisms, algorithms or techniques should be illustrated with significant applications that demonstrate their applicability to real-world problems. Although the *APEM journal* main goal is to publish original research papers, review articles and professional papers are occasionally published.

Fields of interest include, but are not limited to:

Additive Manufacturing Processes
Advanced Production Technologies
Artificial Intelligence
Assembly Systems
Automation
Cutting and Forming Processes
Decision Support Systems
Discrete Systems and Methodology
e-Manufacturing
Fuzzy Systems
Human Factor Engineering, Ergonomics
Industrial Engineering
Industrial Processes
Industrial Robotics
Intelligent Systems
Inventory Management
Joining Processes
Knowledge Management
Logistics
Machine Tools
Machining Systems
Manufacturing Systems
Mechanical Engineering
Mechatronics
Metrology
Modelling and Simulation
Numerical Techniques
Operations Research
Operations Planning, Scheduling and Control
Optimisation Techniques
Project Management
Quality Management
Queuing Systems
Risk and Uncertainty
Self-Organizing Systems
Statistical Methods
Supply Chain Management
Virtual Reality

APEM journal
Advances in Production Engineering & Management **ISSN 1854-6250**
Volume 10 | Number 2 | June 2015 | pp 59–72 Journal home: apem-journal.org
http://dx.doi.org/10.14743/apem2015.2.192 Original scientific paper

Modeling and optimization of parameters for minimizing surface roughness and tool wear in turning Al/SiCp MMC, using conventional and soft computing techniques

Tamang, S.K.[a], **Chandrasekaran, M.**[a,*]

[a]Mechanical Engineering Department, North Eastern Regional Institute of Science and Technology, Nirjuli, India

ABSTRACT

Aluminium alloy with silicon carbide particulate (Al/SiCp) reinforced metal matrix composite (MMC) are used within a variety of engineering applications due to their excellent properties in comparison with non-reinforced alloys. This presented work attempted the development of predictive modeling and optimization of process parameters in the turning of Al/SiCp MMC using a titanium nitride (TiN) coated carbide tool. The surface roughness R_a as product quality and tool wear VB for improved tool life were considered as two process responses and the process parameters were cutting speed v, feed f, and depth of cut d. Two modeling techniques viz., response surface methodology (RSM) and artificial neural network (ANN) were employed for developing R_a and VB predictive models and their predictive capabilities compared. Four different RSM models were tried out viz., linear, linear with interaction, linear with square, and quadratic models. The linear with interaction model was found to be better in terms of predictive performance. The optimum operating zone was identified through an overlaid contour plot generated as a response surface. Parameter optimization was performed for minimizing R_a and VB as a single objective case using a genetic algorithm (GA). The minimum R_a and VB obtained were 2.52 μm and 0.31 mm, respectively. Optimizations of multi-response characteristics were also performed employing desirability function analysis (DFA). The optimal parameter combination was obtained as v = 50 m/min, f = 0.1 mm/rev and d = 0.5 mm being the best combined quality characteristics. The prediction errors were found as 4.98 % and 3.82 % for R_a and VB, respectively, which showed the effectiveness of the method.

ARTICLE INFO

Keywords:
Metal matrix composite
Surface roughness
Tool wear
Response surface methodology
Artificial neural network
Genetic algorithm
Desirability function analysis

**Corresponding author:*
mchse1@yahoo.com
(Chandrasekaran, M.)

Article history:
Received 28 July 2014
Revised 29 March 2015
Accepted 10 April 2015

1. Introduction

The application and use of metal matrix composites (MMC) in manufacturing industries have now become increased due to its improved properties viz., high strength, low weight, high wear resistance, low heat of thermal expansion, etc. [1]. The matrix phase and reinforcement design of the material is responsible for the desired property of MMC. Among different types of MMC available, aluminium based SiC particulate (SiCp) reinforced MMC have found useful application as engineering material [2]. The conversion of these materials into an engineering part or component is obtained by machining through common conventional machining processes like turning, milling, drilling, and grinding. Turning is considered as foremost common machining method because of its ability to machine cylindrical surfaces faster with reasonably good surface finish. Due to hard and abrasive characteristic of reinforcement materials used in MMC the machinability study, development of predictive modeling and optimizing the process parameters have attracted the researchers. Most of the research on MMC machining is concentrated on investigation of cutting tool wear, surface roughness of the machined product, delamination factor of drill holes produced, and metal removal rate during machining.

Yuan and Dong [3] studied on surface finish in precision turning of MMCs using diamond tool. They considered spindle speed, feed rate, cutting angle, volume percentage of reinforcement material as investigating parameters. Davim [4] used Taguchi's orthogonal array and analysis of variance (ANOVA) to investigate the cutting characteristics of MMC (A356/20/SiCp-T6) in turning using polycrystalline diamond (PCD) cutting tool. Cutting velocity, feed rate, and cutting time are considered as input parameters and found that the cutting velocity has the highest physical and statistical influence on the tool wear and cutting power. Feed have high influence on the surface roughness of the component. Muthukrishnan and Davim [5] also conducted an experimental study on turning of Al/SiCp (20 %) MMC using the PCD tool for prediction of the surface roughness and found that the feed rate is a highly influencing parameter. Palanikumar and Karthikeyan [6] have studied on surface roughness using Taguchi method combined with RSM for minimizing the surface roughness in machining GFRP composites with PCD cutting tool. They concluded that fiber orientation and machining time are more influencing parameters on machining for obtaining better surface roughness. Rajasekaran et al. [7] also investigated the influence of surface roughness in turning CFRP composite using cubic boron nitride (CBN) cutting tool and applied fuzzy logic technique for modeling. They found that feed has the greater impact on surface roughness and fuzzy logic model predicts better. The influence of tool wear on machining glass fibre-reinforced plastics (GFRP) composites was investigated by Palanikumar and Davim [8] conducting series of experiments. They used ANOVA technique to assess the influencing parameters.

Chandrasekaran and Devarasiddappa [9] used fuzzy logic for developing surface roughness model for end milling of Al/SiCp metal matrix composite with carbide cutter. They found that the model predicts with an average prediction error of 0.31 % when compared with experimental data. The surface roughness is influenced by feed rate and spindle speed while depth of cut has less influence. In comparing the performance of ANN model with RSM they found that ANN outperforms. Arokiadass et al. [2] also developed surface roughness prediction model for end milling of LM25Al/SiCp MMC using RSM technique. They also have taken influencing parameters as feed rate, spindle speed, depth of cut and SiCp percentage and found that feed rate is the most dominant parameter and depth of cut is of least influence on the surface roughness.

Thiagarajan and Sivaramakrishnan [10] conducted an experimental study for investigating the grindability of Al/SiCp MMC in a cylindrical grinding process. They considered wheel velocity, work piece velocity, feed, depth of cut and SiCp volume fraction percentage as input parameters. They observed that the improved surface roughness and damage free surfaces are obtained at high wheel and workpiece velocity while using white Al_2O_3 grinding wheels. A numerical model based GA optimization methodology has been applied by Davim et al. [11] for determination of optimal drilling conditions in A356/20/p metal matrix composites. The experimental study inferred that the surface finish of the drilled holes increase with increase in feed rate but does not change significantly with variation in cutting speed. Basavarajappa et al. [12] have studied the variation of surface roughness on the drilling of metal matrix composites using carbide tool. They also found that the surface roughness decreases with the increase in cutting speed and increases with the increase in feed rate. Chandrasekaran and Devarasiddappa [13] developed a surface roughness prediction model using artificial neural network (ANN) for grinding of MMC components. The input parameters are wheel velocity, feed, work piece velocity and depth of cut. They found that surface roughness is highly influenced by feed and wheel velocity but least effected by depth of cut. Hocheng and Tsao [14] compared the RSM and radial basis function network (RBFN) for core-center drilling of composite materials. They concluded that for evaluating thrust force RBFN is more practical and predict better than the RSM method. Drilling CFRP composites have investigated by Tsao and Hocheng [15] using Taguchi and neural network methods. They conducted an experiment using Taguchi L_{27} orthogonal array of experiments with feed rate, spindle speed and drill diameter as input parameters. Thrust force and surface roughness produced were output parameters and it has been found that the feed rate and drill diameter are most significant factors for predicting the thrust force. They also confirmed that RBFN model is found to be more effective than multiple regression analysis in predicting the output responses, i.e. surface roughness and thrust force. From review of above literatures the machining investigation on turning Al/SiCp MMC was performed by the researchers. They were mainly considered mainly single response and simultaneous modeling and optimization of surface roughness and tool wear were not attempted. These responses are important for manufacturing industries on the basis of job quality and longer tool life.

In the area of modeling and optimization the researchers were carried out by a number of traditional and soft computing techniques. Application of GA found successful by number of researchers, Mukherjee and Ray [16], and Wang and Jawahir [17]. Öktem et al. [18] used RSM coupled with GA to optimize the cutting conditions for obtaining minimum surface roughness in milling of mold surfaces. For optimizing multi-response characteristics, various researchers use GRA as useful tool. The method does not require mathematical computation and can be applied easily for multi-response problems. Pawade and Joshi [19] have attempted to optimize the high-speed turning of Inconel 718 to optimize machining parameters using grey relational analysis considering cutting speed, feed, depth of cut and edge geometry as input parameters and surface roughness and cutting force as responses. Sahoo and Pradhan [20] carried out an experiment study based on Taguchi L_9 orthogonal array in turning Al/SiC MMC using uncoated carbide tool. Three cutting parameters viz., cutting speed v, feed rate f and depth of cut d were optimized to obtain minimum flank wear and surface roughness. Low and high cutting speed was found as optimum parameter for VB and R_a, respectively. They also developed a linear mathematical model for VB and R_a and found statistically significant as P-value is less than 0.05. In another attempt, Sahoo et al. [21] performed turning experiments on Al/SiC MMC (10 % weight) produced by traditional casting process. Multi-layer coated carbide tool was used to investigate tool wear and surface roughness. They found that cutting speed is the most influencing machining parameter on flank wear and feed rate on surface roughness. They also carried out multi-objective optimization using grey relational grade and found optimum combination as cutting speed at 180 m/min, feed at 0.1 mm/rev, and depth of cut at 0.4 mm. Gopalakannan and Thiagarajan [22] investigated on Al/SiCp MMC using EDM process. Pulse current, gap voltage, pulse on time and pulse off time were considered as input parameters and metal removal rate, electrode wear rate and surface roughness were output parameters. The developed RSM models show good predictive capability. The parameters were optimized using desirability analysis for multiple objectives.

The present work is envisaged to develop a modeling and optimization of machining parameters on the performance characteristics in turning of Al/SiCp MMC using TiN coated cutting tool. Predictive modeling was developed for surface roughness R_a and tool wear VB using RSM and ANN techniques. Machining parameters are optimized for single- and multi-objective case using GA and DFA for minimize R_a and VB or both simultaneously.

2. Development of RSM mathematical model

The statistical tools such as multiple regression analysis, response surface methodology and Taguchi method are widely used for development of conventional predictive modeling. RSM is a collection of mathematical and statistical techniques for empirical model building. It is used for the problems in which an output parameter is influenced by several input parameters and the objective is to optimize the output response. In this work RSM model is developed in order to investigate the influence of machining parameters (i.e., cutting speed v, feed rate f, and depth of cut d on the surface roughness R_a and tool flank wear VB in turning Al/SiCp MMC. All the machining parameters were chosen as independent input variables while desired responses are assumed to be affected by the cutting parameters. The predicted surface roughness (response surface) of turning process can be expressed in term of the investigating independent variables as

$$R_a = Cv^x f^y d^z \tag{1}$$

where R_a is the predicted surface roughness in μm, v is the cutting speed in m/min, f is the feed in mm/rev, and d is the depth of cut in mm. C is the constant and x, y, and z are the exponents to be estimated from experimental results. Eq. 1 is linearized using logarithmic transformation and can be expressed as

$$\ln R_a = x \ln v + y \ln f + z \ln d \tag{2}$$

Eq. 2 is re-expressed into generalized linear model as:

$$y = \beta_0 x_0 + \beta_1 x_1 + \beta_2 x_2 + \beta_3 x_3 = \beta_0 + \sum_i^3 \beta_i x_i \tag{3}$$

where y is true (measured) response surface on logarithmic scale, x_0 is dummy variable and its value is equal to 1, and x_1, x_2, and x_3 are logarithmic transformation of input variables, i.e. cutting speed, feed, and depth of cut, respectively. β_0, β_1, β_2, and β_3 are the parameters to be estimated. If ε is the experimental error between estimated response y' and measured response y then

$$y' = y - \varepsilon = b_0 x_0 + b_1 x_1 + b_2 x_2 + b_3 x_3 \tag{4}$$

where the b values are the estimate of β parameters. The linear model of Eq. 4 is extended as second-order polynomial response surface model (i.e., quadratic model) and is expressed as

$$\begin{aligned} y' = y - \varepsilon = {} & b_0 x_0 + b_1 x_1 + b_2 x_2 + b_3 x_3 + b_{11} x_1^2 + b_{22} x_2^2 + b_{33} x_3^2 + b_{12} x_1 x_2 + b_{13} x_1 x_3 \\ & + b_{23} x_2 x_3 \end{aligned} \tag{5}$$

or

$$y' = b_0 + \sum_{i=1}^{3} b_i x_i + \sum_{i=1}^{3} b_{ii} x_i^2 + \sum_{i=1}^{2} \sum_{j=2}^{3} b_{ij} x_i x_j \tag{6}$$

where b_0 is constant or free term, b_i, b_{ii}, and b_{ij} represent the coefficients of linear, quadratic, and cross product (i.e., interaction) terms. The Eq. 5 can be written as to build the relationship between turning parameters and responses (i.e., surface roughness and tool wear) as

$$y_{R_a} = b_0 + b_1 v + b_2 f + b_3 d + b_{11} v^2 + b_{22} f^2 + b_{33} d^2 + b_{12} x_1 x_2 + b_{13} x_1 x_3 + b_{23} x_2 x_3 \tag{7}$$

$$y_{VB} = b_0 + b_1 v + b_2 f + b_3 d + b_{11} v^2 + b_{22} f^2 + b_{33} d^2 + b_{12} x_1 x_2 + b_{13} x_1 x_3 + b_{23} x_2 x_3 \tag{8}$$

Where b_0 is constant or free term, b_i, b_{ii}, and b_{ij} represent the coefficients of linear, quadratic, and cross product (i.e., interaction) terms. The experimental work carried out by Kılıçkap et al. [23] in turning Al/SiCp MMC using K10 TiN coated cutting tool for investigating surface roughness and tool wear is used in this work. For modeling and analysis of machining parameters RSM model is developed using MINITAB 15® statistical software. Table 1 show various machining parameters used at three levels.

The RSM predictive model is developed using 20 data sets selected based on central composite design (CCD). The CCD experimental design matrix and responses are given in the Table 2. It is used for analyzing the measured response and determining the mathematical model with best fits. The fit summary for surface roughness and tool wear suggests that the quadratic relationship where the additional terms are significant and the model is not aliased.

Table 1 Assignment of levels and parameters

Factor	Units	Symbol	Levels		
			-1	0	1
Cutting speed	m/min	v	50	100	150
Feed	mm/rev	f	0.1	0.2	0.3
Depth of cut	mm	d	0.5	1.0	1.5

Table 2 Experimental result

Sl. No	Cutting speed, v (m/min)		Tool feed, f (mm/min)		Depth of cut, d (mm)		Experimental responses	
	Code (A)	Actual value	Code (B)	Actual value	Code (C)	Actual value	Surface roughness, R_a (μm)	Tool wear, VB (mm)
1	-1	50	1	0.3	1	1.5	4.13	0.601
2	1	150	1	0.3	1	1.5	3.17	1.050
3	-1	50	1	0.3	1	1.5	3.95	0.447
4	0	100	-1	0.1	0	1.0	3.21	0.603
5	0	100	1	0.3	0	1.0	4.03	0.702
6	1	150	1	0.3	-1	0.5	3.47	0.902
7	-1	50	-1	0.1	1	1.5	3.34	0.502
8	0	100	0	0.2	-1	0.5	3.47	0.630
9	0	100	0	0.2	0	1.0	3.40	0.651
10	-1	50	-1	0.1	-1	0.5	3.24	0.327
11	1	150	0	0.2	0	1.0	3.27	0.896
12	0	100	0	0.2	0	1.0	3.40	0.651
13	0	100	0	0.2	0	1.0	3.40	0.651
14	1	150	-1	0.1	0	1.0	3.17	0.623
15	0	100	0	0.2	1	1.5	3.43	0.698
16	1	150	-1	0.1	1	1.5	3.14	0.602
17	0	100	0	0.2	0	1.0	3.40	0.651
18	0	100	0	0.2	0	1.0	3.40	0.651
19	0	100	0	0.2	0	1.0	3.40	0.651
20	-1	50	0	0.2	0	1.0	3.68	0.477

Four different types of RSM mathematical models viz., linear, linear with interaction, and quadratic are obtained for prediction of surface roughness y_{Ra} and tool wear y_{VB} were obtained.

a) Linear model:

$$y_{R_a} = 3.367 - 0.0042v + 2.65f - 0.018d \tag{9}$$

$$y_{VB} = -0.0093 + 0.00344v + 1.045f + 0.1045d \tag{10}$$

b) Linear with interaction models:

$$y_{R_a} = 2.382 + 0.00217v + 8.41f + 0.313d - 0.034vf - 0.00009vd - 1.95fd \tag{11}$$

$$y_{VB} = 0.320 + 0.0018v - 1.63f + 0.127d + 0.018vf - 0.00149vd + 0.612fd \tag{12}$$

c) Linear with square models:

$$y_{R_a} = 3.28 - 0.0026v - 2.13f + 0.88d - 0v^2 + 12.17f^2 - 0.423d^2 \tag{13}$$

$$y_{VB} = -0.053 + 0.0037v + 2.46f - 0.039d - 0v^2 - 3.63f^2 + 0.044d^2 \tag{14}$$

d) Quadratic models:

$$y_{R_a} = 2.55 + 0.0022v + 4.086f + 0.737d - 0.000v^2 + 12.84f^2 - 0.227d^2 - 0.035vf - 0.0009vd - 2.47fd \tag{15}$$

$$y_{VB} = 0.103 + 0.0026v - 0.55f + 0.288d - 4.114f^2 - 0.066d^2 + 0.0203vf - 0.002vd + 0.877fd \tag{16}$$

where *v, f*, and *d* are cutting speed, feed and depth of cut, respectively. From these model equations, it is observed that the factor with highest value of coefficient posses the most dominating effect over the response. Feed has most significant effect over surface roughness and tool wear followed by the depth of cut and cutting speed.

2.1 Checking adequacy of the model

The test of significance of all the models was carried out using analysis of variance (ANOVA) and their predictive capability is analyzed. ANOVA find the influence of machining parameters (*v*, *f*, and *d*) on the total variance of the experimental findings. The test is performed by calculating the ratio between the regression mean square and the mean square error (i.e., F-ratio). The ratio measures the significance of the model in respect of variance of the parameters included in the error term for particular level of significance α. The analysis was carried out at 95 % confidence level and the result is presented in Table 3. The adequacy of the model is decided upon the value of S and coefficient of determination R^2. S value being the measurement of error, it is the smaller value that gives better results. If R^2 approaches unity the response model fits better with the actual data and less difference exists between predicted and actual data. To compare, more precisely adjusted R^2 (Adj R^2) is used, which is adjusted for the degrees of freedom. The closeness of the Adj R^2 with R^2 determines the fitness of the model.

The higher value of R^2 is obtained for linear with interaction model. This shows the predictive capability of *linear with interaction* model is found better and is selected among all models. The model equation used for prediction of surface roughness and tool wear is given in Eq. 11 and Eq. 12, respectively.

Table 3 Test of significance of RSM models

Sl. No.	RSM model	S-Value		R^2		Adj R^2	
		R_a	*VB*	R_a	*VB*	R_a	*VB*
1	Linear	0.15	0.073	76.09	82.51	71.01	79.21
2	Linear with interaction	0.089	0.052	96.00	92.16	94.12	90.00
3	Linear with square	0.15	0.078	80.17	83.59	70.94	76.02
4	Full quadratic	0.089	0.046	94.86	95.63	89.78	91.69

2.2 Contour plots

Fig. 1 shows two dimensional surface plot that shows the effect of influencing parameters on the output responses. Fig. 1(a) reveals that higher cutting speed and lower feed produces better surface finish. Increased feed increases the surface roughness value. This is due to rapid tool movement which deteriorates the quality of the machined surface. The analysis of contour plot shows improved surface roughness is obtained at higher *v* and lower *f*. The combination of parameters with cutting speed at 150 m/min, feed at 0.1 mm/rev, and depth of cut at 0.5 mm produces minimum surface roughness of 3.17 μm.

The tool wear contour plots are shown in Fig. 1(b). Cutting speed is the influencing parameter followed by depth of cut and feed. Higher tool wear is noticed at increased *v*. This is due to increased temperature causing flank wear at tool nose. Tool wear plot shows reduced tool wear is obtained at lower values of *v*, *f*, and *d*. The combination of parameters with cutting speed at 50 m/min, feed at 0.1 mm/rev, and depth of cut at 0.5 mm produces tool wear less than 0.4 mm found as minimum.

The comparison of experimental and RSM prediction for the parameters combination that produces minimum surface roughness and minimum tool wear are presented in the Table 4. However, the optimum region for combined minimization of surface roughness and tool wear is obtained by overlaying contour plot presented in the next subsection.

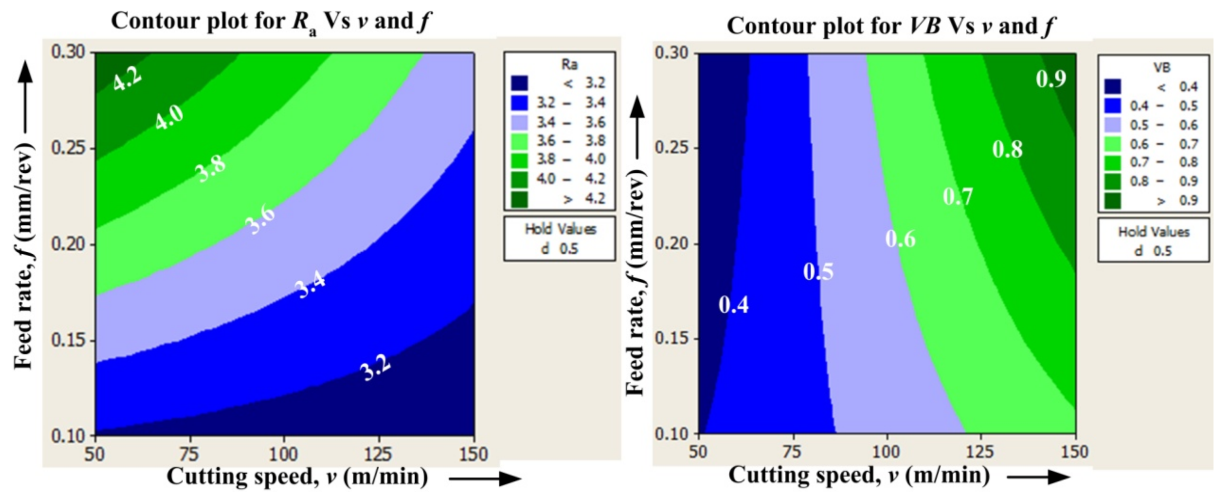

(a) For surface roughness (b) For tool wear

Fig. 1 Contour plots for interaction effect (at d = 0.5 mm)

Table 4 Optimum parameter combination

Sl. No.	Turning parameters (v–f–d)	Expt.	RSM prediction	Error (%)
1	For minimum R_a (150–0.1–0.5)	3.17 µm	3.18 µm	0.32
2	For minimum VB (50 –0.1– 0.5)	0.33 mm	0.38 mm	13.15

2.3 Overlaying contour plot for optimum operating zone

Fig. 2 shows the region for the selection of optimum cutting speed and feed for different value of surface roughness with minimum tool wear. The range of cutting speed as 50-80 m/min and feed as 0.1-0.14 mm/rev with 0.5 mm depth of cut produce surface roughness less than 3.4 µm with tool wear less than 0.5 mm. It may be considered as optimum operating zone. Similar trend have been seen at all values of depth of cut. The method of overlaying contour plot pictorially obtains the optimum operating zone and easy selection of cutting parameters for different values of R_a.

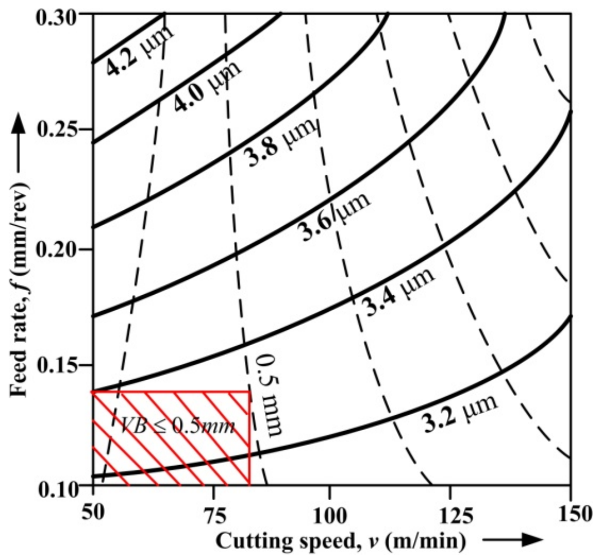

Fig. 2 Optimum operating region

3. Multi-response artificial neural network modeling

Artificial neural network (ANN) is the system that acquire, store and utilize knowledge gained from experience. It is motivated by the biological neurons that work in human brain. Researchers have employed ANN for modeling of machining processes and found that ANN provides reasonable accuracy. The network is built with number of layers (input, hidden and output) having specific number of neurons (also called *nodes*). All the neurons are interconnected with *weights* and *bias* is added at each node. The number of neurons in the input and output layers depend upon input and output parameters of the proposed model. The number of neurons of the hidden layer is decided during network training. The network architecture is trained with the number of real life experimental datasets. Each dataset consists of input parameters and the corresponding output responses. The optimum network is obtained with the selection of appropriate *transfer functions* and number of neurons in the hidden layer. The mean square error between the experimental response and ANN prediction is the criteria for deciding the optimum network architecture. Once network is trained then it is ready for prediction. The trained network is tested with unseen datasets for model validation and the predictive results are compared with experimental results.

The size and selection of training and testing datasets are very crucial in the design of ANN model. There is no well- established formula for finding out the number of training and testing data [24]. Kohli and Dixit [25] have used 19 datasets for training 9 datasets for testing in developing ANN model used for prediction surface roughness in turning process. Nearly 66 % of total experimental data sets are selected is the training phase. The data sets are selected appropriately including extreme datasets (i.e., v_{min}, f_{min}, and d_{min}; v_{max}, f_{max}, and d_{max}). The remaining 34 % datasets were used in the testing phase. The predictive results of the tested data sets are compared with experimental datasets.

In this work, a soft computing based artificial neural network model for predicting surface roughness and tool wear as a function of three input parameters *viz*., cutting speed, feed, and depth of cut is developed. The multi-layer perceptron (MLP) network comprised of an input layer with three neurons, a hidden layer, and an output layer with two neurons. The networks with neurons (nodes) in each layer are interconnected with nodes of the subsequent and preceding layer with synaptic weights. Additionally a bias is added to each neurons of the hidden and output layer. The output of each neuron is obtained by summing up weighted inputs of neuron in preceding layer and its own bias. The output of each neuron in the hidden or output layer is computed by the equation

$$O_j = f(I) = f\left(\sum_{i=1}^{n} w_{ij} x_i + b_j\right) \tag{17}$$

where w_{ij} is the associated weights with j^{th} neurons of the layer and i^{th} neurons of the preceding layer, b_j is the bias of j^{th} neurons, n is the total number of neurons of the preceding layer and f is the appropriate transfer function used. In this work, the ANN model is trained with 19 experimental datasets and tested with eight unseen datasets.

Fig. 3 shows the architecture of two layered feed forward neural network system used in this work. The network is modeled with neural network tool box available in MATLAB® that working on back propagation learning algorithm. The algorithm use gradient decent technique and minimize mean square error (MSE) between actual network outputs with desired output pattern.

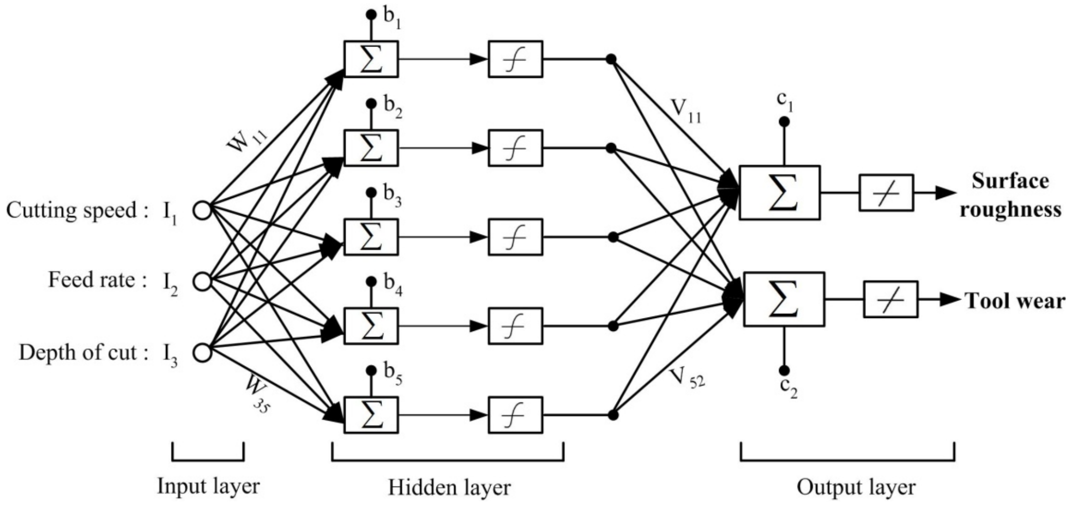

W_{ij} and b_i are weights and bias of hidden layer, respectively
V_{ij} and c_i are weights and bias of output layer, respectively

Fig. 3 ANN architecture

The network is optimized with varying number of neurons in the hidden layer and activation transfer function used so as to obtain minimum MSE. The network architecture with five hidden layer neurons with *tansig* transfer function obtains least MSE of 0.0001 and is considered as optimum network. The output layer uses *purelin* transfer function to evaluate the estimated outputs of surface roughness and tool wear. The validation of the network is performed by predicting surface roughness and tool wear for unseen data sets and ANN prediction is compared with experimental result.

3.1 Comparison of RSM and ANN model performance

The ANN and RSM predicted values for surface roughness and tool wear is compared with the experimental values. The comparison of predictive performance of both the models with the experimental value is given in Table 5. The prediction accuracy *PA* of each datasets was calculated using Eq. 18.

$$PA = \left[1 - \frac{\mathrm{abs}(Expt\_value_i - Model\_pred_i)}{Expt\_value_i}\right] \times 100 \tag{18}$$

Finally, the model accuracy *MA* is computed as the average of individual accuracy on confirmation data set. It is obtained using Eq. 19.

$$MA = \frac{1}{n}\sum_{i=1}^{n}(PA_i) \times 100 \tag{19}$$

The model accuracy of the ANN and RSM model are 95.38 % and 92.90 % for surface roughness and 92.16 % and 91.56 % for tool wear. It can be concluded that the correlation between the prediction of developed models and experimental result is very good. The prediction accuracy in ANN for surface roughness and tool wear is more than 95.00 %. The prediction accuracy for RSM based on linear with interaction model found more than 91.00 % for predicting surface roughness with a maximum PA of 99.69 %. While for tool wear PA is more than 90.0 % with the maximum of 98.64 %. This shows that neural network based prediction model has been found better than the response surface model for turning Al/SiCp metal matrix composite using coated TiN tool.

Table 5 Comparison of ANN and RSM predictive model

Sl. No.	Surface roughness, R_a					Tool wear, VB				
		ANN		RSM			ANN		RSM	
	Expt. (µm)	Pred. (µm)	Pred. acc. (%)	Pred. (µm)	Pred. acc. PA (%)	Expt. (mm)	Pred. (mm)	Pred. acc. PA (%)	Pred. (mm)	Pred. acc. PA (%)
1	3.27	3.48	93.96	3.28	99.69	0.508	0.405	79.72	0.45	88.58
2	3.87	4.16	93.02	3.79	97.93	0.400	0.453	88.30	0.35	87.50
3	4.67	4.49	96.15	4.20	89.93	0.521	0.493	94.63	0.43	82.53
4	4.04	3.59	88.86	3.68	91.08	0.799	0.783	97.99	0.81	98.64
5	4.16	4.37	95.88	3.96	95.19	0.685	0.707	96.89	0.63	91.97
6	3.08	3.00	97.40	3.14	98.08	0.653	0.677	96.46	0.66	98.93
7	3.79	3.78	99.74	3.32	87.59	0.750	0.792	94.70	0.81	92.59
8	4.06	4.02	99.01	3.41	83.99	0.951	0.842	88.54	1.04	91.44
Model accuracy			95.50		92.94	Model accuracy		92.15		91.52

4. Optimization of cutting parameters

The selection of best or right combination of cutting parameters for obtaining optimum process response is still the subject of many studies. In this work the parameter optimization for single as well as multiple objectives is carried out. Optimization for minimum R_a and minimum VB are performed using the non-traditional techniques of genetic algorithm (GA). The optimum parameters are also obtained for simultaneous optimization of R_a and VB using desirability function analysis (DFA).

4.1 Single-objective optimization with GA

GA is one of the popular optimization technique performed by the natural evolution process inspired on the principle of survival of fitness [26]. GA works on the mechanism of genetics and evolution and has been found as a very powerful algorithm for obtaining global minima by Chandrasekaran et al. [27]. In GA the different process parameters are represented either binary or decimal numbers, called as *string* or *chromosome*. A set of chromosomes is called *population*. A population is evolved through several generations using different genetic operations such as reproduction, crossover, and mutation. The best chromosome in the population is identified by the closeness of fitness value with the objective function. The process is repeated till the optimization function converges to the required accuracy after many generations and optimum parameter is obtained. Researchers have found GA as powerful optimization tool/procedure to obtain global optima and the mathematical derivative of the function is not required in this procedure.

In this work, the fitness/objective function of the optimization problem is formulated using the best regression model given in Eq. 20 and Eq. 21 for surface roughness and tool wear, respectively. The formulated single-objective optimization function is given as follows:

$$\begin{aligned}&\text{Minimize } R_a(v,f,d)\\&= Min(2.382 + 0.00217v + 8.41f + 3.313d - 0.034vf - 0.00009vd - 1.95fd)\end{aligned} \tag{20}$$

$$\begin{aligned}&\text{Minimize } VB(v,f,d)\\&= Min(0.320 + 0.0018v - 1.63f + 0.127d + 0.018vf - 0.00149vd + 0.612fd)\end{aligned} \tag{21}$$

The variables of the function are limited by its upper and lower bounds and are given as

$$50 \leq v \leq 150 \tag{22}$$

$$0.1 \leq f \leq 0.3 \tag{23}$$

$$0.5 \leq d \leq 1.5 \tag{24}$$

The problem is optimized using the GA parameters: number of population size was 20, maximum number of iterations was 1000, crossover probability was 0.7 and mutation probability was 0.05. Optimization is performed for obtaining minimum R_a and minimum VB within the range of parameters available and it takes 54 and 61 iterations for R_a and VB, respectively.

4.2 Multi-objective optimization with DFA

The concept of desirability function was first introduced by Derringer and Suich [28] in the year 1980. The method is used for optimization of multiple quality characteristics and found popular among manufacturing industries. The desirability function analysis (DFA) evaluates a *composite desirability value* of the various responses from its *individual desirability*. The method makes use of an objective function called the desirability function and transform an estimated response into a scale-free value d_i called *desirability*. The desirability value varies from 0 to 1. A value of 1 represents the ideal case; 0 indicates that one or more responses are outside their acceptable limits. *Composite desirability* is the weighted geometric mean of the individual desirability evaluated against each response. The parameter settings with maximum composite desirability are considered to be the optimal cutting conditions.

In order to optimize the R_a and VB, DFA is adopted. In DFA optimization of multiple response characteristics is converted into single composite desirability grade [29]. The procedure involves: 1) evaluation of individual desirability d_i, 2) evaluation of composite desirability d_G, and 3) ranking of composite desirability. Experimental data sets based on full factorial design, $3^3 = 27$ data sets are used.

In this work, since both the responses are to be minimized, Eq. 25 is used to evaluate the individual desirability d_i

$$d_i = \left\{ \begin{matrix} 1, y \leq y_{min} \\ \left(\dfrac{y - y_{max}}{y_{min} - y_{max}}\right)^r, y_{min} \leq y \leq y_{max}, r > 0 \\ 0, y \leq y_{max} \end{matrix} \right\} \tag{25}$$

where r is weight, y_{min} and y_{max} are the lower and upper value, respectively.

The next step is to select the parameter combination that will maximize overall desirability d_G using Eq. 26

$$d_G = (d_1 \times d_2 \times d_3 \times \ldots \times d_n)^{1/n} = \left(\prod_{i=1}^{n} d_i\right)^{1/n} \tag{26}$$

where d_i is the individual desirability of the response and n is the number of response in the measure. The desirable ranges from zero to one. If any of the response falls outside the desirability range, the overall function becomes zero. To reflect the difference in the importance of different response the equation can be extended to

$$d_G = d_1^{w1} \times d_2^{w2} \times d_3^{w3} \times \ldots \times d_n^{wn} \tag{27}$$

where the weight w_i satisfies $0 < w_i < 1$, and sum of weights is equal to one. In this work, w_1 *and* w_2 is taken equal as 0.5. Fig. 4 shows the scatter plot of the composite desirability grade for the different set of parameter combination. The larger the grade the better is the multiple performance characteristics. The grade is 0.92 and it corresponds to the first experimental run. The parameter combination as v_1 (50 m/min), f_1 (0.1 mm/rev) and d_1 (0.5 mm) is optimal parameter set. The surface roughness and tool wear predicted by DFA at optimal parameter is 3.24 μm and 0.327 mm, respectively. The confirmation experiments show the surface roughness of 3.41 μm and tool wear of 0.34 mm. The increased surface roughness of 3.24 μm notifies that there is slight loss of quality in simultaneous optimization for multiple responses. However, the confirmation test shows the prediction error percentage is 4.98 % and 3.82 % for R_a and VB, respectively, which shows the effectiveness of the method. Table 6 shows the optimum parameters.

Table 6 Comparison of various optimization techniques

Method	Optimization technique	Optimal parameter combination	Optimal responses
Single-objective optimization	GA	Minimizing R_a: v (134.98 m/min), f (0.1 mm/rev), d (0.5 mm)	R_a = 2.52 µm
		Minimizing VB: v (50 m/min), f (0.21 mm/rev), d (0.5 mm)	VB = 0.31 mm
Multi-objective optimization	DFA	Minimizing R_a and VB: v (50 m/min), f (0.1 mm/rev), d (0.5 mm)	R_a = 3.24 µm VB = 0.327 mm

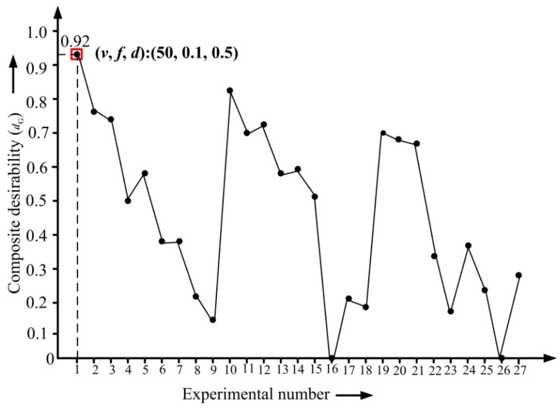

Fig. 4 Scatter plot for composite desirability

5. Conclusion

In this paper the predictive modeling for surface roughness (R_a) and tool wear (VB) in turning Al/SiCp MMC was developed using RSM and ANN. The predictive capability was compared. The three turning parameters viz., cutting speed, feed, and depth of cut are considered as input parameters. The model behavior was analysed through contour plot and optimum operating zone is obtained. The parameters are optimized for single- and multi-response characteristics employing GA and DFA techniques. From the research result the following conclusions are obtained:

1. The surface roughness is highly influenced by feed. Tool wear is influenced by feed and cutting speed. The increase of feed and cutting speed increases VB.
2. Among different RSM models, the linear with interaction model found better in term of predictive performance. The combination of parameters with cutting speed as 150 m/min and feed as 0.1 mm/rev produce minimum surface roughness of 3.3 µm. Minimum tool wear of 0.38 mm is obtained at 50 m/min, feed as 0.1 mm/rev, and depth of cut 0.5 mm. The experimental confirmations show an error of 0.32 % and 13.14 % for R_a and VB, respectively.
3. The response contour plot provides the cutting speed ranges from 50-80 m/min with the feed ranges from 0.1-0.14 mm/rev producing surface roughness less than 3.4 µm with tool wear less than 0.5 mm. It may be considered as the optimum operating zone.
4. Multi-response predictive modeling developed using ANN with 3–5–2 as optimum network architecture providing best prediction accuracy. The model adequacy for surface roughness and tool wear is more than 92 %. On comparison of both RSM and ANN model, the latter is found to be slightly better. ANN shows good generalization ability and found as useful artificial intelligence tool for monitoring machining process.
5. Parameter optimization for single objective using GA obtains minimum R_a and VB as 2.52 µm and 0.31 mm, respectively. DFA based multi-response optimization obtain optimal parameter combination as v_1 (cutting speed, 50 m/min), f_1 (feed, 0.1 mm/rev) and d_1 (depth of cut 0.5 mm) having highest desirability grade of 0.92. Confirmation test shows the percentage of error as 4.98 % and 3.82 % for R_a and VB , respectively, which shows the effectiveness of the method.

Acknowledgement

The authors are thankful to the anonymous reviewers for their useful comments and suggestions to improve the quality of the manuscript. The authors also thankful to Astt. Prof. Raju Borthakur (HSS Department, NERIST) for his kind help in the preparation of the manuscript.

References

[1] Allison, J.E., Cole, G.S. (1993). Metal-matrix composites in the automotive industry: Opportunities and challenges, *Journal of the Minerals, Metals & Materials Society*, Vol. 45, No. 1, 19-24, doi: 10.1007/BF03223361.

[2] Arokiadass, R., Palanirajda, K., Alagumoorthi, N. (2011). Predictive modeling of surface roughness in end milling of Al/SiCp metal matrix composite, *Archives of Applied Science Research*, Vol. 3, No. 2, 228-236.

[3] Yuan, Z.J., Geng, L., Dong, S. (1993). Ultra precision machining of SiCw/Al composites, *CIRP Annals – Manufacturing Technology*, Vol. 42, No. 1, 107-109, doi: 10.1016/S0007-8506(07)62403-2.

[4] Davim, J.P. (2003). Design of optimisation of cutting parameters for turning metal matrix composites based on the orthogonal array, *Journal of Materials Processing Technology*, Vol. 132, No. 1-3, 340-344, doi: 10.1016/S0924-0136(02)00946-9.

[5] Muthukrishnan, N., Davim, J.P. (2009). Optimization of machining parameters of Al/SiC-MMC with ANOVA and ANN analysis, *Journal of Materials Processing Technology*, Vol. 209, No. 1, 225-232, doi: 10.1016/j.jmatprotec.2008.01.041.

[6] Palanikumar, K., Karthikeyan, R. (2006). Optimal machining conditions for turning of particulate metal matrix composites using Taguchi and response surface methodologies, *Machining Science and Technology,* Vol. 10, No. 4, 417-433, doi: 10.1080/10910340600996068.

[7] Rajasekaran, T., Palanikumar, K., Vinayagam, B.K. (2011). Application of fuzzy logic for modeling surface roughness in turning CFRP composites using CBN tool, *Production Engineering*, Vol. 5, No. 2, 191-199, doi: 10.1007/s11740-011-0297-y.

[8] Palanikumar, K., Davim, J.P. (2009). Assessment of some factors influencing tool wear on the machining of glass fibre-reinforced plastics by coated cemented carbide tools, *Journal of Materials Processing Technology*, Vol. 209, No. 1, 511-519, doi: 10.1016/j.jmatprotec.2008.02.020.

[9] Chandrasekaran, M., Devarasiddappa, D. (2012). Development of predictive model for surface roughness in end milling of Al-SiCp metal matrix composites using fuzzy logic, *World Academy of Science, Engineering and Technology*, Vol. 6, No. 7, 928-933.

[10] Thiagarajan, C., Sivaramakrishnan, R., Somasundaram, S. (2011). Cylindrical grinding of SiC particles reinforced aluminium metal matrix composites, *ARPN Journal of Engineering and Applied Sciences*, Vol. 6, No. 1, 14-20.

[11] Davim, J.P., Reis, P., António, C.C. (2004). Experimental study of drilling glass fiber reinforced plastics (GFRP) manufactured by hand lay-up, *Composites Science and Technology*, Vol. 64, No. 2, 289-297, doi: 10.1016/S0266-3538(03)00253-7.

[12] Basavarajappa, S., Chandramohan, G., Prabu, M., Mukund, K., Ashwin, M. (2007). Drilling of hybrid metal matrix composites – Workpiece surface integrity, *International Journal of Machine Tools and Manufacture*, Vol. 47, No. 1, 92-96, doi: 10.1016/j.ijmachtools.2006.02.008.

[13] Chandrasekaran, M., Devarasidappa, D. (2014). Artificial neural network modeling for surface roughness prediction in cylindrical grinding of Al-SiCp metal matrix composites and ANOVA analysis, *Advances in Production Engineering & Management,* Vol. 9, No. 2, 59-70, doi: 10.14743/apem2014.2.176.

[14] Hocheng, H., Tsao, C.C. (2005). The path towards delamination-free drilling of composite materials, *Journal of Materials Processing Technology*, Vol. 167, No. 2-3, 251-264, doi: 10.1016/j.jmatprotec.2005.06.039.

[15] Tsao, C.C., Hocheng, H. (2008). Evaluation of thrust force and surface roughness in drilling composite material using Taguchi analysis and neural network, *Journal of Material Processing Technology*, Vol. 203, No. 1-3, 342-348, doi: 10.1016/j.jmatprotec.2006.04.126.

[16] Mukherjee, I., Ray, P.K. (2006). A review of optimization techniques in metal cutting processes, *Computers & Industrial Engineering*, Vol. 50, No. 1-2, 15-34, doi: 10.1016/j.cie.2005.10.001.

[17] Wang, X., Jawahir, I.S. (2005). Optimization of multi-pass turning operations using genetic algorithms for the selection of cutting conditions and cutting tools with tool-wear effect, *International Journal of Production Research*, Vol. 43, No. 17, 3543-3559, doi: 10.1080/13629390500124465.

[18] Öktem, H., Erzurumlu, T., Kurtaran, H. (2005). Application of response surface methodology in the optimization of cutting conditions for surface roughness, *Journal of Materials Processing Technology*, Vol. 170, No. 1-2, 11-16, doi: 10.1016/j.jmatprotec.2005.04.096.

[19] Pawade, R.S., Joshi, S.S. (2011). Multi-objective optimization of surface roughness and cutting forces in high-speed turning of Inconel 718 using Taguchi grey relational analysis (TGRA), *The International Journal of Advanced Manufacturing Technology*, Vol. 56, No. 1-4, 47-62, doi: 10.1007/s00170-011-3183-z.

[20] Sahoo, A.K., Pradhan, S. (2013). Modeling and optimization of Al/SiCp MMC machining using Taguchi approach, *Measurement*, Vol. 46, No. 9, 3064-3072, doi: 10.1016/j.measurement.2013.06.001.

[21] Sahoo, A.K., Pradhan, S., Rout, A.K. (2013). Development and machinability assessment in turning Al/SiCp-metal matrix composite with multilayer coated carbide insert using Taguchi and statistical techniques, *Archives of Civil and Mechanical Engineering*, Vol. 13, No. 1, 27-35, doi: 10.1016/j.acme.2012.11.005.

[22] Gopalakannan, S., Thiagarajan, S. (2014). Optimization of machining parameters for EDM operations based on central composite design and desirability approach*, Journal of Mechanical Science and Technology*, Vol. 28, No. 3, 1045-1053, doi: 10.1007/s12206-013-180-x.

[23] Kılıçkap, E., Çakır, O., Aksoy, M., İnan, A. (2005). Study of tool wear and surface roughness in machining of homogenised SiC-p reinforced aluminium metal matrix composite, *Journal of Materials Processing Technology*, Vol. 164-165, 862-867, doi: 10.1016/j.jmatprotec.2005.02.109.

[24] Dixit, P.M., Dixit, U.S. (2008). *Modeling of metal forming and machining processes by finite element and soft computing methods,* Springer-Verlag, London.

[25] Kohli, A., Dixit, U.S. (2005). A neural-network-based methodology for the prediction of surface roughness in a turning process, *The International Journal of Advanced Manufacturing Technology*, Vol. 25, No. 1-2, 118-129, doi: 10.1007/s00170-003-1810-z.

[26] Goldberg, D.E. (1989). *Genetic algorithms in search, optimization and machine learning*, Addison-Wesley Longman Publishing Co., Boston, Massachusetts.

[27] Chandrasekaran, M., Muralidhar, M., Murali Krishna, C., Dixit, U.S. (2010). Application of soft computing techniques in machining performance prediction and optimization: A literature review, *The International Journal of Advanced Manufacturing Technology*, Vol. 46, No. 5-8, 445-464, doi: 10.1007/s00170-009-2104-x.

[28] Derringer, G., Suich, R. (1980). Simultaneous optimization of several response variables, *Journal of Quality Technology*, Vol. 12, No. 4, 214-219.

[29] Naveen Sait, A., Aravindan, S., Noorul Haq, A. (2009). Optimisation of machining parameters of glass-fibre-reinforced plastic (GFRP) pipes by desirability function analysis using Taguchi technique, *The International Journal of Advanced Manufacturing Technology*, Vol. 43, No. 5-6, 581-589, doi: 10.1007/s00170-008-1731-y.

APEM journal

Advances in Production Engineering & Management
Volume 10 | Number 2 | June 2015 | pp 73–86
http://dx.doi.org/10.14743/apem2015.2.193

ISSN 1854-6250
Journal home: apem-journal.org
Original scientific paper

Predictive analysis of criterial yield during travelling wire electrochemical discharge machining of Hylam based composites

Mitra, N.S.[a,*], Doloi, B.[b], Bhattacharyya, B.[b]

[a]Production Engineering Department, Haldia Institute of Technology, Haldia, India
[b]Production Engineering Department, Jadavpur University, Kolkata, India

A B S T R A C T

Travelling wire electrochemical discharge machining (TW-ECDM) has great potential for machining advanced non-conducting materials such as zirconia, alumina, silicon nitride, diamond glass, rubies and composites such as FRP etc. Composite materials possess higher strength, stiffness, and fatigue limits which enable structural design more flexible than with conventional metals. Over recent years precision machining of composite materials has gained in importance. The presented research paper includes a description of an indigenously developed TW-ECDM set-up for performing experiments on composite materials such as fibre reinforced plastic. This paper also presents analyses of machining parameters such as material removal rate and radial overcut for different input parameters such as pulse on time, frequency of power supply, applied voltage, concentration of electrolyte and wire feed rate. Taguchi method-based optimization analysis was also done for achieving minimum radial overcut and maximum material removal rate during the cuttings of grooves on Hylam based fibre reinforced composites. Multiple regression models were also established for both material removal rate and radial overcut by considering the more important process parameters for cutting grooves on Hylam based fibre reinforced composites. Finally, a back propagation neural network was applied for predicting the responses and those predictions are compared with the experimental results.

A R T I C L E I N F O

Keywords:
TW-ECDM
Groove cutting
Fibre reinforced composites
Taguchi method
Artificial neural nets

**Corresponding author:*
nsmitra@rediffmail.com
(Mitra, N.S.)

Article history:
Received 2 March 2014
Revised 24 March 2015
Accepted 26 March 2015

1. Introduction

The researchers are urgently looking for techniques to keep up with the development of new materials such as engineering ceramics and composites etc. [1]. The demand for machining hard and brittle materials is steadily increasing in many applications. Presently various non-traditional machining processes are available but the inherent problems associated with these processes are thermal damage due to large heat affected zone, high tool wear rate, low material removal rate, high surface roughness, poor dimensional accuracy etc. Precision machining of fibre reinforced plastic (FRP) is also a challenge. Hylam is a mixture of cellulose, adhesive based on modified epoxy resin and hardener, the tensile strength and Young's modulus of which vary with fibre content. It has important properties like electrical insulation, moisture resistance and corrosion resistance. Fibre reinforced composites are widely accepted in structural and non-structural applications like household goods, switchboards and control panels. With conventional machining the laminated structure of FRP is damaged and machined surface becomes rough. To cope up with these challenges, manufacturing scientists are making use of the combined hybrid machining process, which also reduces some adverse effects of individual process. Electrochemical arc machining (ECAM) is found to have scope for electrically conductive materials. Electrochemical discharge machining (ECDM) [2-4] can be used for electrically conducting engineering materials. Further the traditional method of slicing ceramics depends upon the grinding force of hard particles and grinding results in micro-cracks. For slicing electrically non-conducting materials, Traveling wire electrochemical discharge machining (TW-ECDM) is a viable option [5, 6]. TW-ECDM is a complex combination of ECM and wire-EDM. In TW-ECDM, a pulsed DC power is supplied between the wire and auxiliary electrode. In this process, the conducting wire is used as cathode and auxiliary electrode is used as anode. In this process, the conducting wire is always in contact with the non-conducting workpiece material. As the pulsed DC power is supplied, hydrogen and vapour bubbles are formed and accumulated near the wire surface. With the further increase of applied voltage, the electric spark discharge occurs between the wire and the electrolyte across the insulating layers of gas bubbles. As the job surface is kept in the sparking zone, material is removed mainly due to melting and vaporization of the workpiece material. The feasibility study of machining FRP with ECSM was made [7]. Machining of non-conducting materials such as alumina, glass is still a major problem and although ECSM is most popular machining technique for those material it has certain difficulties. If ordinary cutting tools are used, the results are not so good like electrochemical spark abrasive drilling of alumina and glass [8]. An attempt was made to measure the true time varying current of ECSM to reveal the basic mechanism, temperature rise and material removal [9]. Spark assisted chemical engraving (SACE) had been investigated using current/voltage measurement and photographs [10]. A preliminary study of a pulse discriminating system was carried out for developing a control strategy of ECDM [11]. A thermal model was developed for the calculation of the material removal rate during ECSM [12]. Micromachining of non-conductive ceramics and composites has been attempted by ECSM and TW-ECSM [13-18]. Parametric analysis of TW-ECDM process using developed setup has also been attempted [19].

From the above past research activities it is understood that focus was mainly on the TW-ECDM or ECDM process and developing a model based on statistical experimental design. But no attempt was made to determine the dominant and recessive parameters of the process and there was no attempt to reduce the cost while increasing the quality. Also there were very few efforts in predicting the output from a set of input variables. Further FRP is a new material which is extremely important for application.

Keeping the above past research activities in view, this research paper includes Taguchi method based parametric analysis on TW-ECDM cutting of groove on flat surfaces of Hylam-based fibre reinforced composite workpiece. Multiple nonlinear regression analysis has also been done to find out the empirical relationship between the responses and the most important process parameters of TW-ECDM. The verification experiments have been performed to compare between predicted results and experimental results. Finally a 3-9-1 feed forward back propagation neural network has been used to predict the responses for different parametric combinations and those are compared with the actual results.

2. Experimental setup of TW-ECDM system

TW-ECDM system has been developed to carry out experimental investigation and optimal analysis of machining characteristics of TW-ECDM process. Fig. 1 shows the schematic diagram of the TW-ECDM setup. The TW-ECDM system consists of subsystems such as mechanical hardware unit, control limit for wire feeding and electrical power supply unit. The photographic view of the setup is shown in Fig. 2.

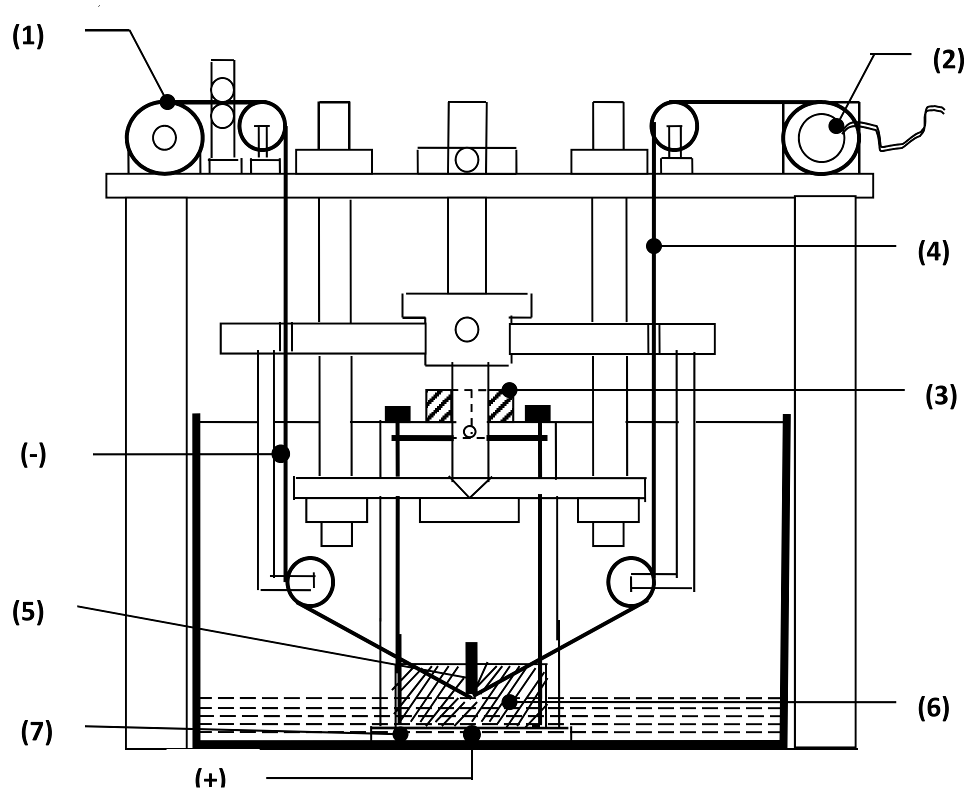

Legends: (1) Input spool, (2) Output spool with stepper motor, (3) Pulley for gravity feed mechanism, (4) Wire electrode (cathode), (5) Workpiece in vertical position, (6) Workpiece holding Perspex piece, (7) Auxiliary electrode (anode)

Fig. 1 Schematic view of the TW-ECDM setup

(a) (b)

Fig. 2 Photographic view of the TW-ECDM setup along with control units

Mechanical hardware unit consists of wire feeding unit, wire positioning unit, job holding unit and these units are fitted inside the main machining chamber. The wire feeding unit consists of input spool, output spool and a set of intermediate pulleys. The output spool is coupled with a motor and as the motor rotates it draws the wire out of the input spool through the intermediate pulleys. The wire feeding unit feeds the wire continuously as per the required feed rate. The wire positioning unit consists of three parts such as wire guide unit, wire guide positioning unit and effective wire length adjusting mechanism. It helps to keep the wire in touch with the work-piece. The job holding unit holds the job and controls the inter electrode gap. It also helps to facilitate the contact between the hydrogen bubbles evolved and the workpiece. The movement of the job holding unit can be controlled by means of gravity feed mechanism. Minimum gap between wire and auxiliary electrode is kept at 30 mm. For the purpose of experiment, the inter-electrode gap is fixed at 45 mm. The entire assembly is fitted in a machining chamber made up of Perspex which is kept in the lower platform of a two-storied wooden table. A hole is made at the bottom of the machining chamber and the lower platform of the wooden table, through which a lower Perspex piece with a central hole is attached. On the other side of the Perspex piece a plastic nozzle and gate valve assembly is attached. With this assembly a polyvinyl chloride made water spraying pipe is attached. The open end of the pipe is immersed in a big size plastic pail which collects the used electrolyte. Aqueous solution of KOH salt is used as electrolyte. The micro controller based stepper motor unit is a menu based operational system where both the speed and direction of rotation of stepper motor can be varied. The feed rate of wire can be set from 0.05-0.4 m/min. The rpm of the stepper motor can be varied from 1 to 80. The input voltage of the stepper motor is 12 V and the current to the stepper motor is 4 A. The traveling wire electrochemical discharge machining system demands for voltage of 5-150 V, current of 0-7 A and frequency of 50-2000 Hz depending on the rate of material removal and other machining criteria. Keeping in view of this need a pulsed dc power supply is developed. It provides the supply voltage from 0-100 V.

3. Planning for experimentation

Keeping in view the fact of properly controlling the machining performances, the objective of the present research has been to study the main influencing factors among pulse on time as a percentage of total time (A), frequency (B), applied voltage (C), concentration of electrolyte (D) and wire feed rate (E) affecting the responses like material removal rate (MRR) and radial overcut (ROC). Taguchi method based robust design principles [20] have been used for the purpose of employing a L_{25} (5^5) orthogonal array to study the effect of process parameters. Each factor is assigned 5 levels as listed in Table 1.

Considering the required properties like tensile strength, melting point of the material etc. brass wire of 0.25 mm diameter was chosen as cathode or tool. Hylam based fibre reinforced composites of 3 mm thickness were used as workpiece. Solution of KOH salt was used as electrolyte. The weight of the job before and after machining was measured and the difference was divided by machining time to get the material removal rate. For each experiment the time taken was 10 min. Olympus STM6 optical measuring microscope was used to measure the radial overcut. The weight of the workpiece before and after machining was measured by SARTORIUS GC103 digital balance. Each experiment is replicated 3 times to observe the readings of material removal rate and radial overcut.

Table 1 Factors with their levels

Control Factors	Levels				
	1	2	3	4	5
Pulse on Time – A, (%)	50	55	60	65	70
Frequency of power supply – B, (Hz)	55	65	75	85	95
Applied voltage – C, (V)	30	35	40	45	50
Electrolyte concentration – D, (%)	10	15	20	25	30
Wire feed rate – E, (mm/min)	50	125	175	225	300

4. Taguchi method based optimal parametric analysis

Taguchi method of robust design makes use of orthogonal arrays to determine the effect of various process parameters based on analysis of signal to noise (S/N) ratio (η). Mathematically it can be computed as

$$\eta = -10 \log (MSD) \tag{1}$$

where *MSD* is the mean square deviation and commonly known as quality loss function. Depending on experimental objective the quality loss function can be of three types: smaller the better, larger the better and nominal the best. The values of signal to noise ratio were calculated for material removal rate based on larger the better quality principle and for radial overcut based on smaller the better principle. The data summary in terms of S/N ratios are given in Table 2, and the results of analysis of variance for material removal rate and radial overcut are shown in Table 3 and Table 4, respectively.

Table 2 Data summary

Experiment No.	Factor Levels					S/N ratios (dB)	
	A	B	C	D	E	MRR	ROC
1	1	1	1	1	1	-11.7005	22.9748
2	1	2	2	2	2	-10.1728	17.2024
3	1	3	3	3	3	-9.1186	18.3443
4	1	4	4	4	4	-7.3306	19.0156
5	1	5	5	5	5	-7.3306	14.8945
6	2	1	2	3	4	-10.1728	19.4939
7	2	2	3	4	5	-9.1186	19.3315
8	2	3	4	5	1	-6.5580	10.2290
9	2	4	5	1	2	-7.7443	17.3933
10	2	5	1	2	3	-10.4576	23.6091
11	3	1	3	5	2	-7.5380	16.5948
12	3	2	4	1	3	-8.1737	18.7860
13	3	3	5	2	4	-7.1309	19.5762
14	3	4	1	3	5	-10.1728	18.5624
15	3	5	2	4	1	-7.1309	16.0269
16	4	1	4	2	5	-7.9588	17.8588
17	4	2	5	3	1	-5.8486	15.8097
18	4	3	1	4	2	-7.5350	18.8619
19	4	4	2	5	3	-7.1309	17.2656
20	4	5	3	1	4	-8.4043	17.7882
21	5	1	5	4	3	-4.5830	14.1993
22	5	2	1	5	4	-7.3306	19.4123
23	5	3	1	2	5	-8.4043	20.7242
24	5	4	3	2	1	-6.1961	15.1890
25	5	5	4	3	2	-5.1927	16.4205

Table 3 ANOVA for MRR

Factors	Degrees of freedom	Sum of squares	Mean square	F-Value	Contribution (%)
TON – A	4	25.2875	6.3219	13.1378	35.9804
Frequency – B	4	1.9085	0.4771	0.9915	2.7155
Applied voltage – C	4	27.5150	6.8788	14.2951	39.1498
Concentration – D	4	11.7040	2.9260	6.0806	16.6531
WFR – E	4	3.7470	0.9368	1.9468	5.3314
Error	4	0.1193	0.0298	-	0.1698
Pooled error	12	5.7748	0.4812	-	8.2170
Total	24	70.2813	2.9284	-	100.0000

Table 4 ANOVA for ROC

Factors	Degrees of freedom	Sum of squares	Mean square	F-Value	Contribution (%)
TON – A	4	4.8940	1.2235	0.2436	2.5509
Frequency – B	4	2.1930	0.5483	0.1902	1.1430
Applied voltage – C	4	61.8995	15.4749	3.0807	32.2634
Concentration – D	4	41.9480	10.4870	2.0877	21.8642
WFR – E	4	27.7315	6.9329	1.3802	14.4543
Error	4	53.1908	13.2977	---	27.7242
Pooled error	12	60.2778	5.0232	---	31.4181
Total	24	191.8568	7.9940	---	100.0000

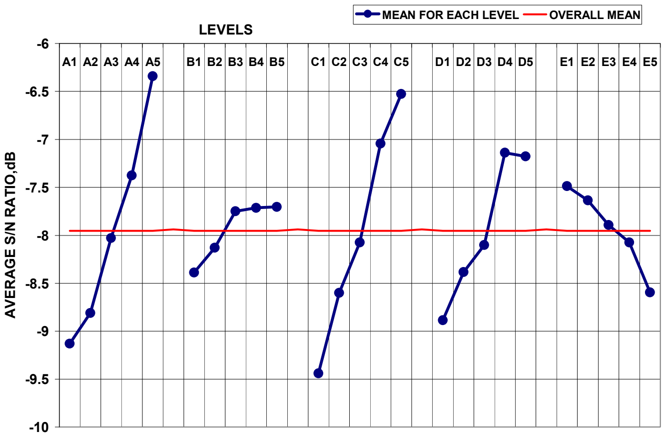

Fig. 3 S/N ratio plot for MRR

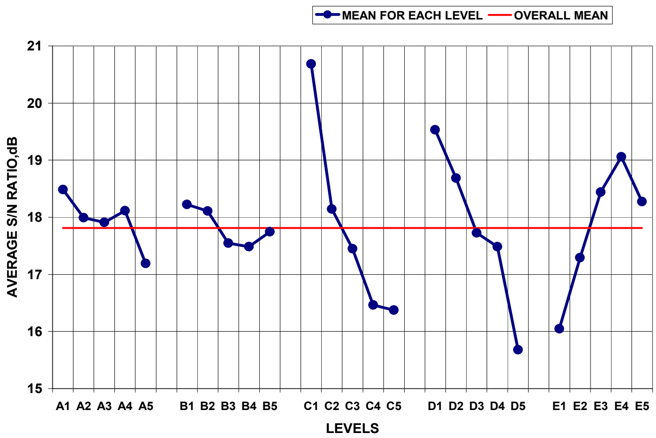

Fig. 4 S/N ratio plot for ROC

The corresponding factor effects at different levels for material removal rate and radial overcut in terms of S/N ratios are plotted in Fig. 3 and Fig. 4, respectively.

From S/N ratio plot it has been observed that for achieving maximum MRR the optimal parametric setting is $A_5B_5C_5D_4E_1$, i.e. pulse on time as 70 % of the total pulse duration, pulse frequency of 95 Hz, applied voltage of 50 V, electrolyte concentration of 25 % by weight and wire feed rate of 50 mm/min. For achieving minimum radial overcut the optimal parametric setting is $A_1B_1C_1D_1E_4$, i.e. pulse on time as 50 % of the total pulse duration, pulse frequency of 55 Hz, applied voltage of 30 V, electrolyte concentration of 10 % by weight and wire feed rate of 225 mm/min. Comparing the variances and degrees of contribution for each control factor it is realized that pulse on time, applied voltage and concentration of electrolyte are the most influencing factors for material removal rate and applied voltage, concentration of electrolyte and wire feed rate are most influencing factors for radial overcut. The percentage improvements in the optimum condition based on signal to noise ratio is listed in Table 5.

Table 5 Improvements based on S/N ratio

Responses	Starting condition (dB)	Predicted optimum condition (dB)	Percentage improvement (dB)
MRR	-11.5831	-3.4484	70.23
ROC	21.7309	24.7422	13.86

Table 6 Results of verification experiment

Responses	Optimal parametric settings					Values
	A	B	C	D	E	
MRR (mg/min)	70	95	50	25	50	0.620
ROC (mm)	50	55	30	10	225	0.065

It is observed that the percentage improvement of material removal rate is 70.23 % and of radial overcut is 13.86 %. The results of verification experiments are shown in Table 6.

5. Development of empirical models

The empirical models have been developed by non-linear multiple regression analysis on the basis of L_{25} (5^5) orthogonal array of robust design. In the analysis based on Taguchi method it was found that for material removal rate the most significant parameters are pulse on time as a percentage of total time, applied voltage and concentration of electrolyte. Empirical model for material removal rate is developed by considering the most significant process parameters. Empirical model for radial overcut is also developed by considering the most significant process parameters such as applied voltage, concentration of electrolyte and wire feed rate. The mathematical relationship between material removal rate and most significant process parameters is established as follows:

$$Y = 0.4170 + 0.0326X_1 + 0.0264X_2 + 0.0206X_3 + 0.0013X_1^2 - 0.0004X_2^2 - 0.0041X_3^2 \quad (2)$$

where $X_1 = \frac{(TON-60)}{5}$, $X_2 = \frac{(AV-40)}{5}$, $X_3 = \frac{(CONC-20)}{5}$ and Y = MRR (mg/min)

The mathematical relationship between radial overcut and the corresponding significant process parameters is as follows:

$$Y = 0.0651 + 0.0157X_1 + 0.0150X_2 - 0.0051X_3 - 0.0043X_1^2 + 0.0033X_2^2 + 0.0062X_3^2 \quad (3)$$

where $X_1 = \frac{(AV-40)}{5}$, $X_2 = \frac{(CONC-20)}{5}$, $X_3 = \frac{(WFR-175)}{25}$ and Y = ROC (mm)

As pulse on time increases more pulse energy is obtained per spark resulting in more heat generation during melting and hence material removal rate also increases. As applied voltage increases more pulse energy is obtained per spark and more heat is generated during melting and material removal rate also increases. More concentration of electrolyte means more conductivity of electrolyte and extent of chemical reaction also increases with the concentration of electrolyte. As degree of chemical reaction increases, more hydrogen vapour bubbles are formed resulting in more sparking and more heat generation in melting resulting in more material removal rate.

At low value of applied voltage, pulse energy per spark is less resulting in less heat generation during sparking. Rate of melting of material also decreases. As applied voltage increases energy per spark also increases resulting in more generation of heat during melting and radial overcut also increases. With the increase in concentration of electrolyte, radial overcut first increases and then decreases. At less value of concentration, vapour blanketing of wire is incomplete and irregular sparking causes more radial overcut. At moderate value of concentration extent of chemical reaction is more resulting in proper vapour blanketing of wire and more controlled and localized sparking resulting in minimum overcut. At higher values of concentration extent of chemical reaction is still greater than that of at a moderate electrolyte concentration and uneven and thicker blanketing of wire causes unstable and violent sparking and hence radial overcut is also maximum. As wire feed rate increases radial overcut first increases and then decreases. This is due to the reason that initially when chemical reaction occurs hydrogen bubbles are evolved and those bubbles form an insulating layer around the wire electrode. Then due to uniform sparking more materials are melted and hence radial overcut is also more. As wire feed rate increases, bubbles are swept away with the wire thus adversely affecting the sparking and hence less material is melt resulting in less radial overcut.

In the two equations derived above the resultant overall effect of all the above mentioned parameters are reflected.

Applied voltage was found to be most influential process parameter of TW-ECDM. Fig. 5 and Fig. 6 show the actual and estimated values of MRR and ROC for different levels of applied voltage.

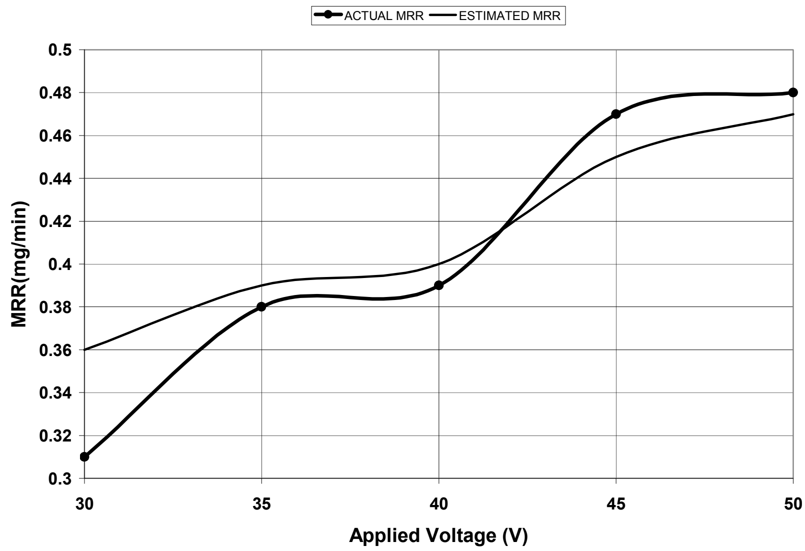

Fig. 5 Comparison of actual MRR and estimated MRR based on model

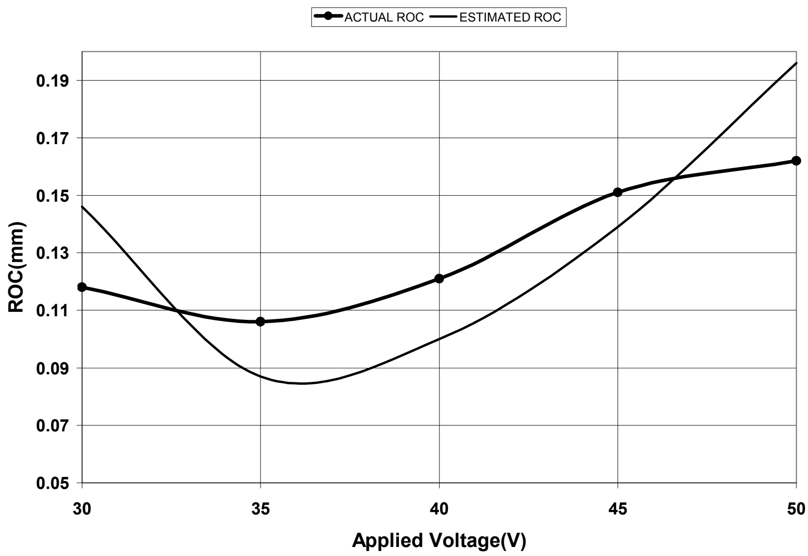

Fig. 6 Comparison of actual ROC and estimated ROC based on model

6. Artificial neural network

An artificial neural network (ANN) is a massively parallel distributed processor made up of signal processing units, which has a natural propensity for storing experiential knowledge and making it available for use. A neural network derives its computing power through, first, its massively parallel distributed structure and, second, its ability to learn and therefore generalize. Generalization means producing reasonable outputs from inputs not encountered during learning or training. These two information processing capabilities make it possible for neural networks to solve large scale problems that are currently intractable. In practice however neural network cannot provide solution by working individually. Rather they need to be integrated into a consistent system engineering approach. Specifically a complex problem of interest is decomposed into a number of relatively simple tasks and neural networks are assigned to a subset of the tasks that match their inherent capabilities. Different kinds of ANN architectures are single layer feed forward network, multilayer feed forward network, recurrent network etc. In multilayer feed forward network one or more hidden layers are present. The free parameters of a neural network are adapted through a process of stimulation by the environment in learning. Learning may be error correction learning, memory based learning, Hebbian learning, competitive learning, Boltzmann learning etc. according to methods. The model of environment in which the neural network operates is known as learning paradigm. Learning process may be supervised or unsupervised. Supervised learning algorithms employ an external reference signal and generate an error signal by comparing the reference with the obtained response. Based on the error signal the synaptic weights are modified. In back propagation neural network we have used back propagation supervised learning algorithm.

7. Prediction using ANN

In the feedforward backpropagation neural network model or perceptron there is an input layer, an output layer and one or more hidden layer. Each input layer has an input and an output. Like input layer each hidden layer and output layer has an input and an output. Weights are applied between outputs of input layer and inputs of hidden layer and and between output of hidden layer and inputs of output layer.

For input layer if linear transfer function is used, then

$$[O]_I = [I]_I \tag{4}$$

If hidden layer neurons are connected by synapses to input neurons then

$$[I]_H = [V][O]_I \tag{5}$$

where $[V]$ is weight matrix applied to output of input layer.

The unipolar sigmoidal transformation function is used for transformation of input of hidden layer to output of hidden layer. The unipolar sigmoidal transformation function is given by

$$O_{Hp} = \frac{1}{1 + e^{-\lambda I_{Hp}}} \tag{6}$$

where λ is sigmoidal.

For transformation of output of hidden layer to input of output layer is accomplished by

$$[I]_O = [W][O]_H \tag{7}$$

where [W] is weight matrix applied to output of hidden layer.

The transformation of input of output layer to output of output layer is given by the following unipolar sigmoidal function

$$O_{Op} = \frac{1}{1 + e^{-\lambda I_{Op}}} \tag{8}$$

After the output is obtained it is compared with the target value which is the experimental value and error is calculated as

$$E = \frac{1}{2}(T - O)^2 \tag{9}$$

where E is error, T is target value, and O is output value.

Based on the error and the learning algorithm, by trial and error methods the weights are changed again and again and the neural network is trained using the weights. A large number of iterations are performed until the values of error are sufficiently small and the required results are obtained.

Here a 3-9-1 feed forward back propagation network is used to analyze the performance separately for each output. The values of the machining parameters are taken as input and actual experimental values are treated as target values. The outputs of each experimental parametric setting are compared with the target values and errors are calculated. In this model of multilayer perceptron, linear activation function is used in input layer while unipolar sigmoidal function is used in both hidden layer and output layer. For material removal rate the value of sigmoidal gain is taken as 0.125 and for radial overcut the value of sigmoidal gain is taken as 0.130. Using programming through MATLAB the outputs and errors are generated. Table 7 shows the predictions for material removal rate while Table 8 shows the predictions for radial overcut.

Fig. 7 shows the relation between ANN values and experimental values for MRR and Fig. 8 shows relation between ANN values and experimental values for ROC. Combining the tables and the figures it can be concluded that this theoretical model can satisfactorily explain the complex experimental behaviour of the TW-ECDM process although there is still sufficient room for improvements. Fig. 9 shows variations in theoretical and experimental values in different experiments for MRR while Fig. 10 shows variations in theoretical and experimental values in different experiments for ROC. Fig. 11 shows microscopic view of one machined workpiece.

Table 7 Prediction for MRR using ANN

Experiment No.	Theoretical values	Actual values	Errors	Experiment No.	Theoretical values	Actual values	Errors
1	0.5665	0.2600	0.0470	14	0.5671	0.3100	0.0331
2	0.5669	0.3100	0.0330	15	0.5673	0.4400	0.0081
3	0.5671	0.3500	0.0236	16	0.5673	0.4000	0.0140
4	0.5672	0.4300	0.0094	17	0.5673	0.5100	0.0016
5	0.5673	0.4300	0.0094	18	0.5673	0.4200	0.0108
6	0.5671	0.3100	0.0331	19	0.5673	0.4400	0.0081
7	0.5672	0.3500	0.0236	20	0.5672	0.3800	0.0175
8	0.5673	0.4700	0.0047	21	0.5674	0.5900	0.0002
9	0.5671	0.4100	0.0123	22	0.5673	0.4300	0.0094
10	0.5669	0.3000	0.0356	23	0.5672	0.3800	0.0175
11	0.5673	0.4200	0.0109	24	0.5673	0.4900	0.0030
12	0.5671	0.3900	0.0157	25	0.5673	0.5500	0.0001
13	0.5672	0.4400	0.0081				

Table 8 Prediction for ROC using ANN

Experiment No.	Theoretical values	Actual values	Errors	Experiment No.	Theoretical values	Actual values	Errors
1	0.5929	0.071	0.1362	14	0.5935	0.118	0.1130
2	0.5934	0.138	0.1037	15	0.5933	0.158	0.0948
3	0.5935	0.121	0.1116	16	0.5935	0.128	0.1083
4	0.5935	0.112	0.1159	17	0.5934	0.162	0.0931
5	0.5935	0.180	0.0855	18	0.5934	0.114	0.1149
6	0.5935	0.106	0.1188	19	0.5935	0.137	0.1042
7	0.5935	0.108	0.1178	20	0.5935	0.129	0.1079
8	0.5934	0.308	0.0407	21	0.5935	0.195	0.0794
9	0.5934	0.135	0.1051	22	0.5935	0.107	0.1183
10	0.5934	0.066	0.1391	23	0.5935	0.092	0.1257
11	0.5935	0.148	0.0992	24	0.5933	0.174	0.0879
12	0.5935	0.115	0.1145	25	0.5934	0.151	0.0979
13	0.5935	0.105	0.1193				

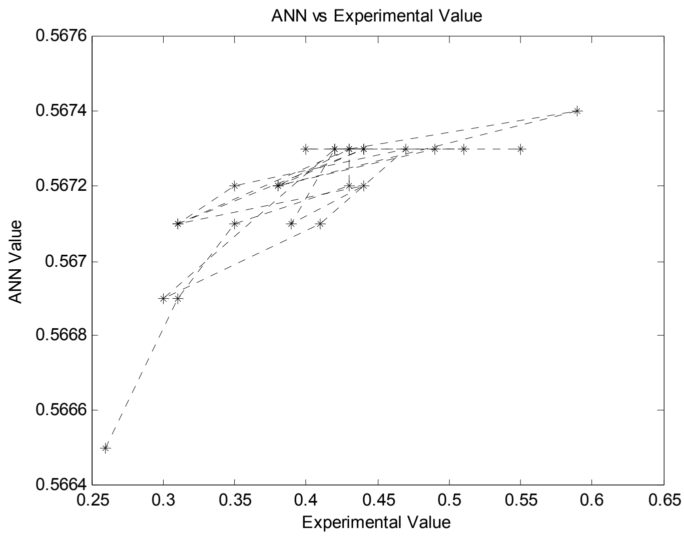

Fig. 7 Relation between ANN values and experimental values in MRR

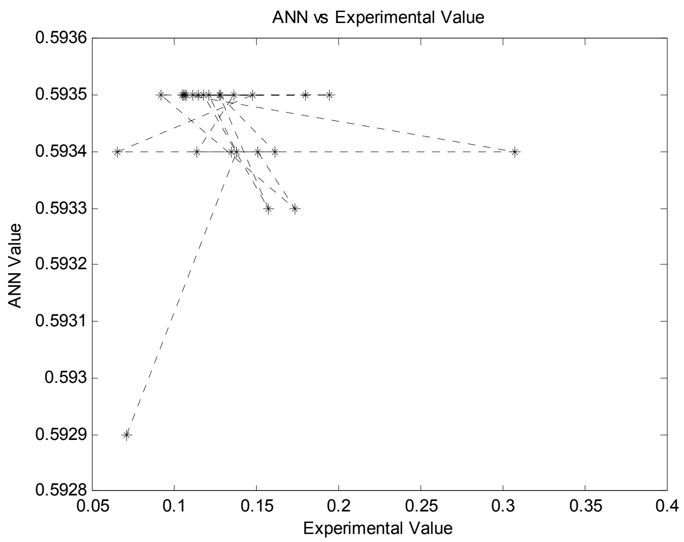

Fig. 8 Relation between ANN values and experimental values in ROC

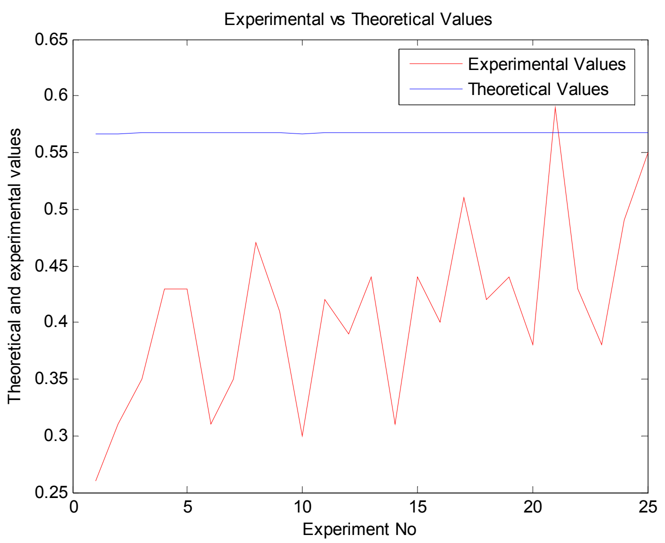

Fig. 9 Variation in MRR for different experiments

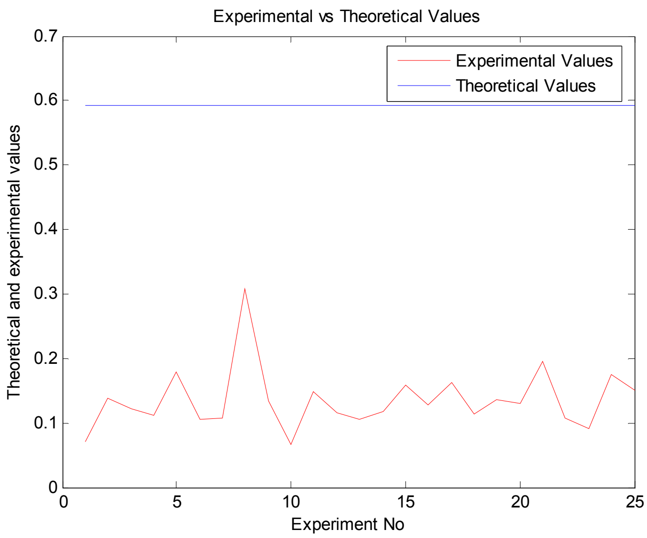

Fig. 10 Variation in ROC for different experiments

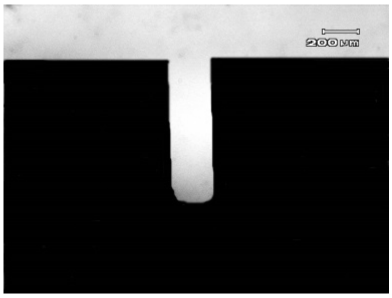

Fig. 11 Microscopic view of machined workpiece

8. Conclusion

The TW-ECDM system has ability to perform the machining operation such as cutting electrically non-conductive engineering materials like fibre reinforced composites. From the observed results and analysis on TW-ECDM process, it is clear that for maximum material removal rate (MRR) the parametric combination is pulse on time as 70 % of the total time, pulse frequency of 95 Hz, applied voltage of 50 V, electrolytic concentration of 25 % by weight and wire feed rate of 225 mm/min. For minimum radial overcut (ROC) the optimal parametric combination is obtained as pulse on time as 50 % of the total pulse time, frequency of 55 Hz, applied voltage of 30 V, electrolyte concentration of 10 % by weight and wire feed rate of 225 mm/min. From the analysis of variance pulse on time, applied voltage and concentration of electrolyte are found as more significant process parameters affecting material removal rate and applied voltage, concentration of electrolyte and wire feed rate as more significant process parameters affecting radial overcut. Earlier researches on ECDM and TW-ECSM focused mainly on developing experimental setup for machining ceramics and composites etc. and determining the nature of pulse, having an insight of material removal mechanism and mathematical modelling of the process to determine the response of the outputs against individual process parameters, but very few attempts have been made to classify the process parameters as dominant or recessive. Verification experiment has also been conducted to test the validation of experiments based on orthogonal array and it was proved that improvement in the machining output has occurred. The authors have earlier conducted research on TW-ECDM [19] but the scope of that research was only confined to single response and multi-response optimization though a hybrid method of Taguchi method and principal component analysis (PCA) and it also revealed the complex interaction between the process parameters. But that analysis did not predict the behaviour of the responses against process parameters and no mathematical relation have been developed. In the current research an analysis has been made enlightening the non-linear relationship of a single response like material removal rate and radial overcut. From the plot of material removal rate and radial overcut against applied voltage it was observed that in case of material removal rate the response increases with applied voltage and experimental values matches with estimated values to maximum extent between 35 V and 45 V where as both experimental and estimated values show similar trend of change between 35 V and 45 V. Thus it is observed that if material removal rate increases, radial overcut will also increase thus putting a restriction on arbitrarily increasing the material removal rate and reasonably good result can be obtained by machining with 35 V to 45 V, although maximum MRR is obtained for 50 V and minimum ROC is obtained for 30 V. Owing to the complexity arising out of using multiple parameters together, an effort has been made to fit a feed forward back propagation neural network model between the parameters and responses and after sufficient training of the network the results obtained showed similar results as in the case of multiple regression analysis. This effort has never been made in earlier researches. Prediction using ANN shows that as actual values increases the predicted values also increases and the errors indicate the degree of fitness of the ANN. Prediction by both multiple regression and ANN gives an idea that best value of machining with respect to MRR will occur at the higher end of the parameter ranges, which exactly matches with the earlier research by the authors. This necessitates the redesign of electrical and electronic circuits of the present setup. Also different kind of optimization of the responses can be attempted with the same set of parameters and with the same experimental setup. Different kind of electrolyte solution and different work materials can also be used with the present setup with modification. The present setup can also be modified for micromachining of ceramics and composites.

Acknowledgement

The authors acknowledge the financial support of UGC, New Delhi for Centre for Advanced Studies (CAS) phase III programme in the Production Engineering Department of Jadavpur University, Kolkata.

References

[1] Bhattacharyya, B., Doloi, B.N., Sorkhel, S.K. (1999). Experimental investigations into electrochemical discharge machining (ECDM) of non-conductive ceramic materials, *Journal of Materials Processing Technology,* Vol. 95, No. 1-3, 145-154, doi: 10.1016/S0924-0136(99)00318-0.

[2] Basak, I., Ghosh, A. (1997). A mechanism of material removal in electrochemical discharge machining: A theoretical model and experimental verification, *Journal of Materials Processing Technology*, Vol. 71, No. 3, 350-359, doi: 10.1016/S0924-0136(97)00097-6.

[3] Jain, V.K., Adhikary, S. (2008). On the mechanism of material removal in electrochemical spark machining of quartz under different polarity conditions, *Journal of Materials Processing Technology*, Vol. 200, No. 1-3, 460-470, doi: 10.1016/j.jmatprotec.2007.08.071.

[4] Chak, S.K., Rao, P.V. (2007). Trepanning of Al_2O_3 by electro-chemical discharge machining (ECDM) process using abrasive electrode with pulsed DC supply, *International Journal of Machine Tools and Manufacture*, Vol. 47, No. 14, 2061-2070, doi: 10.1016/j.ijmachtools.2007.05.009.

[5] Jain, V.K., Rao, P.S., Choudhary, S.K., Rajurkar, K.P. (1991). Experimental investigations into travelin wire electrochemical spark machining (TW-ECSM) of composites, *Journal of Manufacturing Science and Engineering*, Vol. 113, No. 1, 75-84, doi: 10.1115/1.2899625.

[6] Peng, W.Y., Liao, Y.S. (2004). Study of electrochemical discharge machining technology for slicing non-conductive brittle materials, *Journal of Materials Processing Technology*, Vol. 149, No. 1-3, 363-369, doi: 10.1016/j. jmatprotec.2003.11.054.

[7] Tandon, S., Jain, V.K., Kumar, P., Rajurkar, K.P. (1990). Investigation into machining of composites, *Precision Engineering*, Vol. 12, No. 4, 227-238, doi: 10.1016/0141-6359(90)90065-7.

[8] Jain, V.K., Choudhury, S.K., Ramesh, K.M. (2002). On the machining of alumina and glass, *International Journal of Machine Tools and Manufacture*, Vol. 42, No. 11, 1269-1276, doi: 10.1016/S0032-3861(02)00241-0.

[9] Kulkarni, A., Sharan, R., Lal, G.K. (2002). An experimental study of discharge mechanism in electrochemical discharge machining, *International Journal of Machine Tools and Manufacture*, Vol. 42, No. 10, 1121-1127, doi: 10.1016/S0890-6955(02)00058-5.

[10] Wüthrich, R., Hof, L.A. (2006). The gas film in spark assisted chemical engraving (SACE) – A key element for micro-machining applications, *International Journal of Machine Tools and Manufacture*, Vol. 46., No. 7-8, 828-835, doi: 10.1016/j.ijmachtools.2005.07.029.

[11] Mediliyegedara, T.K.K.R., De Silva, A.K.M., Harrison, D.K., McGeough, J.A. (2004). An intelligent pulse classification system for electrochemical discharge machining (ECDM) – A preliminary study, *Journal of Material Processing Technology*, Vol. 149, No. 1-3, 499-503, doi: 10.1016/j.jmatprotec.2004.04.002.

[12] Bhondwe, K.L., Yadava, V., Kathiresan, G. (2006). Finite element prediction of material removal rate due to electro-chemical spark machining, *International Journal of Machine Tools and Manufacture*, Vol. 46, No. 14, 1699-1706, doi: 10.1016/j.ijmachtools.2005.12.005.

[13] Manna, A., Kundal, A. (2011). Micromachining of nonconductive Al_2O_3 ceramic on developed TW-ECSM setup, *International Journal of Manufacturing, Materials and Mechanical Engineering*, Vol. 1, No. 2, 46-55, doi: 10.4018/ijmmme.2011040103.

[14] Mallick, B., Sarkar, B.R., Doloi, B., Bhattacharyya, B. (2013). Parametric analysis of travelling wire electrochemical discharge machining process, *Reason – A Technical Journal*, Vol. 12, 93-101.

[15] Jawalkar, C.S., Sharma, A.K., Kumar, P. (2012). Micromachining with ECDM: Research potentials and experimental investigations, *International Journal of Mechanical and Aerospace Engineering*, Vol. 6, 7-12.

[16] Manna, A., Narang, V. (2012). An experimental investigation during micro-machining of e-glass fibre epoxy composite on developed electrochemical spark machining setup, *International Journal of Manufacturing, Materials and Mechanical Engineering*, Vol. 2, No. 2, 46-60, doi: 10.4018/ijmmme.2012040103.

[17] Cao, X.D., Kim, B.H., Chu, C.N. (2013). Hybrid micromachining of glass using ECDM and micro grinding, *International Journal of Precision Engineering and Manufacturing*, Vol. 14, No. 1, 5-10, doi: 10.1007/s12541-013-0001-6.

[18] Mitra, N.S, Doloi, B., Bhattacharyya, B. (2014). Analysis of traveling wire electrochemical discharge machining of Hylam based composites by Taguchi method, *International Journal of Research in Engineering and Technology*, Vol. 2, No. 2, 223-236.

[19] Manna, A., Kundal, A. (2015). An experimental investigation on fabricated TW-ECSM setup during micro slicing of nonconductive ceramic, *The International Journal of Advanced Manufacturing Technology*, Vol. 76, No. 1-4, 29-37, doi: 10.1007/s00170-013-5145-0.

[20] Phadke, M.S. (1989). Quality engineering using robust design, Prentice Hall, Englewood Cliffs, New Jersey, USA.

APEM journal

Advances in Production Engineering & Management
Volume 10 | Number 2 | June 2015 | pp 87–96
http://dx.doi.org/10.14743/apem2015.2.194

ISSN 1854-6250
Journal home: apem-journal.org
Professional paper

Increasing student motivation and knowledge in mechanical engineering by using action cameras and video productions

McCaslin, S.E.[a], Young, M.[b,*]

[a]Department of Mechanical Engineering, The University of Texas at Tyler, Texas, United States of America
[b]Department of Management and Marketing, The University of Texas at Tyler, Texas, United States of America

A B S T R A C T

Action cameras were used in a material science class laboratory setting for improving student motivation and understanding of material failure mechanisms. The design, implementation, and student perceptions were examined when using cameras. The students recorded video footage of destructive material testing using GoPro Hero action cameras in order to evaluate material failure and develop a video presentation. The use of action cameras allowed students to view and record their experiments without the risk of damage to a more expensive camera, view their experiments in slow motion, and improve technical communication skills. An assessment of the innovation was conducted through student feedback and existing performance measures related to continuous quality improvement. Students participated in developing a grading rubric for video laboratory presentations. Five criteria in order of importance were content, clarity, organization, format, and creativity. The students' surveys were positive regarding increased understanding of course material and improved technical communication skills. The students were satisfied with the variety of laboratory experiments. They perceived increases in their abilities to share technical information through a medium other than written reports. Implications included needing more training in camera usage, editing, and video production techniques in order to improve the learning process. This innovation could be extended to other engineering and management classes.

A R T I C L E I N F O

Keywords:
Mechanical engineering
Student learning
Materials management
Action camera
Video production

**Corresponding author:*
myoung@uttyler.edu
(Young, M.)

Article history:
Received 17 June 2014
Revised 26 January 2015
Accepted 12 February 2015

1. Introduction

1.1 Technology and engineering education

In the past two decades, more and more attention has been devoted to the evaluation and appraisal of technology in the classroom. Likewise, studies have examined methods of instruction, student motivation, and improved learning. Such studies suggest that technology and hands-on experiences in the classroom may improve learning and motivation. The classroom innovation using technology described in this study is using GoPro Hero2 action cameras as an additional project for the required course, Materials Science and Manufacturing.

The mechanical engineering course has a significant laboratory portion which involves destructive material testing. Goals of this project in utilizing GoPro HD Hero2 action camera kits were to: (1) stimulate interest and enthusiasm in the laboratory material; (2) increase understanding of material failures; and (3) improve technical communication skills. This paper will discuss the design, implementation, and results of adding this technology to an engineering laboratory setting.

1.2 Background

Students had commented previously that performing repeated material tests had become monotonous. In addition, similar tests had to be run on different types of materials to understand how failure mechanisms differ among material types. Therefore, this initiative included both new and informative methods in conducting the experiments. A major premise of the study was not all laboratory reports in the industry are limited to paper. However, with the lower costs of digital cameras and videos plus available easy-to-use editing software, presenting results with video productions has become feasible.

This study focused on using the GoPro Hero action cameras to assess student learning, motivation, and teambuilding. GoPro Hero 2 cameras were purchased to enable 120 frames per second digital recording of destructive material tests, such as impact, tensile, and compression and bending tests. Students used the footage to further evaluate the damage mechanisms and obtain additional data. In addition, the project provided students both visual and traditional data to review and analyse.

A specific objective of this initiative was to prepare students to present scientific results in a format that goes beyond professors and classmates. To this end, students took the footage from the experiments and prepared video laboratory reports. These videos were uploaded to a dedicated YouTube channel. Also, students participated in developing a rubric to enhance an effective evaluation of their team projects.

Student surveys indicated that students generally did indeed benefit from the experience with some exceptions. Accordingly, implementation, findings, and evaluation of the camera project in a materials science laboratory setting are examined.

2. Using technology in a materials science laboratory setting

2.1 Literature review

Goodhew and Bullough [1] believed a goal in a materials science laboratory should not only be that the students correctly obtain a proper measurement but also encouraged to do something useful with their results. As new technology is made available to educators and students, it is possible to find new ways to encourage students to take a closer look at what they are studying, whether it is in the classroom or in the laboratory.

Davies and Ringer [2] examined a flexible learning studio with equipment for both studying and preparing presentations for materials science engineering students. He recognized that modern engineering students need skills not only to obtain results but present them to others as well.

Pinder-Grover et al. [3] used screencasts to overcome the difference in academic backgrounds and interests of students coming into a large materials science course. Likewise, Laoui and O'Donoghue [4] implemented a multimedia virtual learning environment to achieve a similar goal. Another web-based approach was developed by Kurt, Kubat, and Oztumel using a conceptual model of a virtual materials testing laboratory simulation for students [5].

The applications of GoPro cameras in research have been numerous in several areas over the past few years. For example, the action camera was used to capture the remote control monitoring of a robotic arm [6], and motion capture in microgravity [7]. Kindt used a head-mounted GoPro camera to gain a better understanding of the student's point of view during a class lecture [8].

Tugrul (2012) studied using a camera in the classroom The research conducted in a marketing course in a private university in Turkey found video-recorded presentations in the learning environment were highly effective in learning outcomes and enriching the education [9].

Schultz reported examples of using video productions in other disciplines including the use of student-produced videos in management classes. Interacting with the management content was believed to give students a greater chance of understanding and synthesizing the material [10].

Although video assignments have been used in the classroom in other disciplines, none have implemented the particular needs of mechanical engineering materials laboratories. Cochrane and O'Donoghue found that engineering students created video productions to present to their peers [11]. Armstrong, Tucker, and Massad investigated an innovative project where students developed and produced podcasts, giving students hands-on experience with modern tools [12].

A recent study hypothesized that in engineering classes, student learning is more effective with interactive activities than constructive, passive activities. The researchers measured student knowledge and understanding of materials science and engineering concepts. The results showed that students scored higher in all post-tests while participating in interactive activities [13].

2.2 Purpose of material science and manufacturing laboratory

Materials Science and Manufacturing, a required course in the mechanical engineering program, consists of two hours of lecture and one hour of laboratory per week. The course description is as follows: "Introduction to materials science including the structure of metals and polymers, the testing of mechanical properties of materials, the relationship between material properties, structure and processing techniques, and the capabilities and limitations of modern manufacturing methods."

The laboratory portion of the course allows students the opportunity to gain "hands-on" experience with materials testing, focusing on tensile, impact, hardness, and bending tests. Inherent within this type of experience is learning to create professional, high-quality reports. Three of the 12 course learning objectives related to the innovation are to:

1. Analyse the effect of heat treatment on metal alloys.
2. Perform standard hardness, tensile, and impact tests on metals and polymers.
3. Present experimental results in laboratory reports.

Traditional testing allowed students to perform numerous tests of material properties using only visual aids at normal camera speeds using cellular phone cameras. However, due to the destructive nature of some of the lab tests, the recording may contain risks for both students and camera.

3. The action camera experiment

3.1 The action camera GoPro Hero2

This pilot study implemented a high definition GoPro HD Hero2 action camera kit in order to capture more than just numbers in the materials testing lab session. According to CNET editors, the GoPro HD Hero2 has a glass lens, a mini-USB port for charging, a 2.5 mm microphone input, a full-size SD card slot, an HDMI video output, and a 1,100 mAh lithium ion battery [14]. In addition, it ships with a clear polycarbonate waterproof housing with spring-loaded waterproof buttons giving the user access to all buttons needed for recording and modifying settings [14]. The camera kit used contained housings to facilitate its secure attachment to almost anything from a helmet to a piece of swinging lab equipment (see Fig. 1).

Fig. 1 GoPro HD Hero2 action camera (Source: GoPro website)

The innovative aspects of this approach consisted of using a lower cost, more student-friendly medium to capture relatively high-speed videos. While the video quality may not be as excellent as a 1000 fps, multi-thousand dollar camera, it seemed sufficient to perform experiments in material failure and to capture exciting visual results.

3.2 Usage in the laboratory

The action cameras captured 120 fps footage of material failure in impact tests, tensile tests, and tensile tests of metal and plastic specimens (including heat treated metal specimens). Cameras were set up to record the failure of the material for all three types of tests and placed in a position which allowed ease in switching off and on during the test. Yet, because of its small size, its position was assured a safe area from the equipment. Two similar setup recorded impact tests were: (1) camera faces the specimen as it comes out of the impact tester; and (2) camera records the trajectory of the specimen as it leaves the impact tester. For example, its usage is described in connection with a Charpy V-notch impact test, using a pendulum testing.

Students were tasked with not only recording the impact strength indicated by the impact tester, but to (1) estimate the speed of the specimen as it left the tester and (2) comment on the breakage of the specimen as it left the tester. This data was then supplemented with digital photos of the before and after specimen.

To maintain a smooth operation of the laboratory sessions, the teams took turns performing and recording their experiments. To achieve the simultaneous recording of the experiment from multiple angles, a WiFi BacPac + ComboKit allowed the recordings to begin at the same time while removing the students from hazardous moving equipment (e.g., the impact tester pendulum arm) as recording begins.

4. Creating video productions

4.1 Student teamwork

In order to increase student interest in video production, a dedicated YouTube channel was created [15]. This channel included videos of the impact test of a metal specimen from two different views and recorded at 120 fps, in lieu of the 30 fps that is typical of a standard digital video camera.

An in-class demonstration on editing footage in Windows MovieMaker was given [16]. In addition, students were provided information on downloading the free trial of Camtasia Studio from TechSmith, which supports integration of PowerPoint slides with video and imaging [17]. Each laboratory team chose a team name and was assigned a Blackboard team page for sharing and editing files. Their team names were used with the laboratory videos posted on YouTube to protect privacy.

After the experiment was performed, the video files were uploaded to the team page on Blackboard. If issues arose with the file exchange on Blackboard, the file was posted to another online file sharing system. Next, the student teams completed the video lab editing and then submitted their video productions for grading.

4.2 Student expectations and evaluation

Students were given the opportunity to assist in developing the rubric for effective grading of the video productions. They agreed that the most important weights for the evaluation should be content (45 %), clarity (30 %), organization (10 %), format (9 %), and creativity (5 %). The video production grade was assigned as a team grade. Also, this same rubric was used during the second year of using the cameras and is shown in Table 1.

Table 1 Rubric for video laboratory reports

Criteria	Novice	Competent	Proficient
Content	*0–10 points* Missing over ½ the required content	*11–30 points* Includes at least half of the required content	*31–45 points* Contains all the required content
Clarity	*0–5 points* Excessive use of technical jargon without explanation, or incorrect explanation	*6–20 points* Use of technical terms fully explained with correct explanation, but requires a strong background in science to understand	*20–30 points* Technical terms fully explained with correct explanation understandable to someone without a physics background
Organization	*0–1 point* Poorly organized	*2–6 points* Organization is present, but flow is not logical	*7–10 points* Shows evidence of careful organization with logical flow
Format	*0–2 points* Unprofessional formatting	*3–7 points* Professional formatting, but minimal effort put into appearance	*8–9 points* Professional formatting with considerable effort put into appearance
Creativity	*0–1 points* Minimal creativity exhibited	*2–4 points* Some level of creativity, but showing little evidence of thought or skill	*5 points* High level of creativity, showing evidence of thought and skill

(Source: Developed by instructor and students in the Materials Science and Manufacturing class)

4.3 Impact testing and video production

The first video laboratory covered impact testing and required students to use the video footage to estimate the speed of the specimen as it flew out of the impact testing machine. This requirement assisted the students in viewing video footage as part of the actual experimental data, rather than as a visual supplement to data.

Next, students recorded video footage for an experiment of their own choosing. The following tests were performed:

- impact testing of a polymer specimen,
- tensile testing of a polymer specimen,
- tensile testing of an aircraft bolt,
- bending tests of steel,
- compression tests of tests of steel,
- bending test of heat treated Damascus steel.

Each team video submitted for the second video laboratory was shown in class. Students commented on all team videos and were shared via the Blackboard team page and used in final grading.

4.4 Videos on YouTube

When the submitted videos were posted on YouTube, keywords were impact testing, material testing, bending testing, and Hero GoPro. Accordingly, the videos became more useful to a wide variety of audiences. A screenshot of the videos posted on the dedicated YouTube channel is shown in Fig. 2.

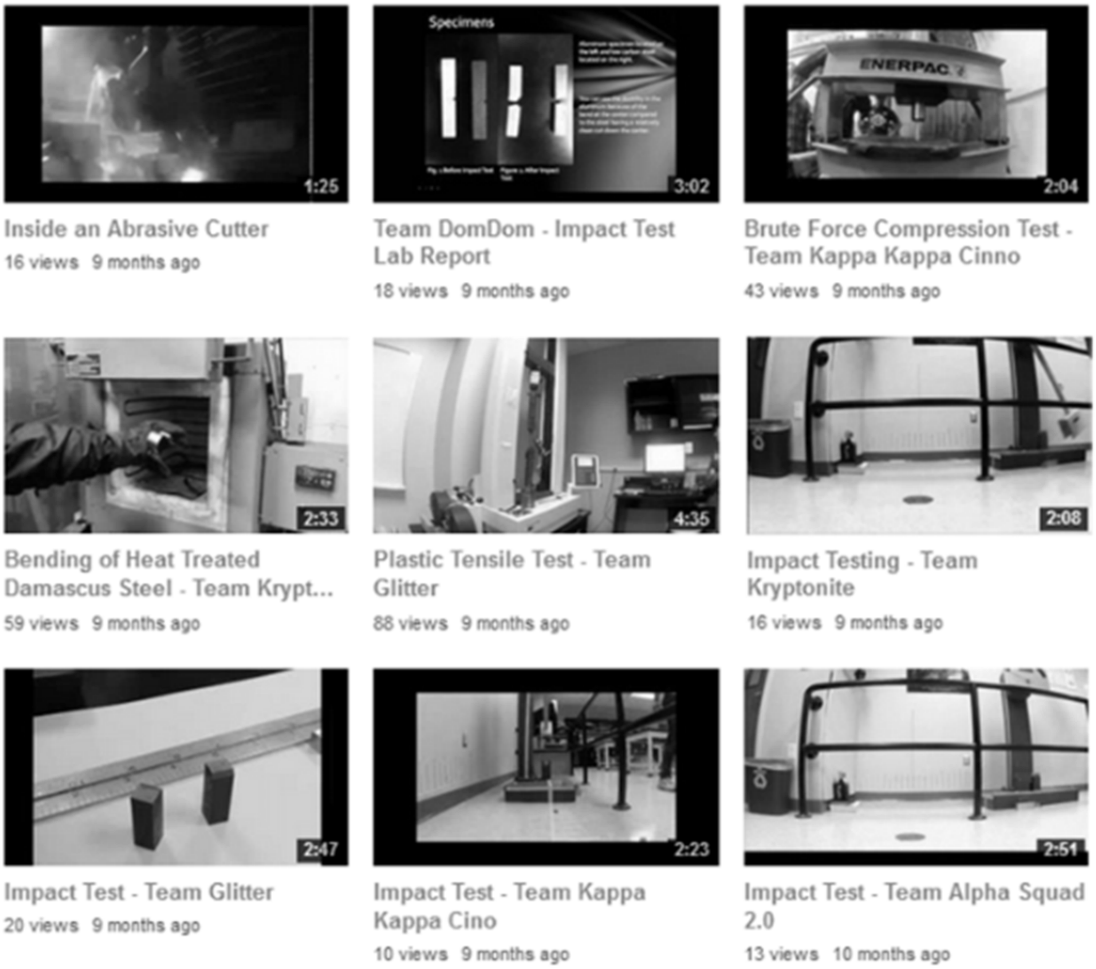

Fig. 2 Video team production presentations on YouTube

5. Assessment of the action camera experiment

Three types of assessment were used to determine the effectiveness of this innovation. They were (1) student surveys from laboratory; (2) departmental surveys on student perception of understanding of course learning objectives; and (3) mechanical engineering faculty ratings according to student performance and accreditation standards.

The last two methods are an inherent part of the accreditation process of the Department of Mechanical Engineering by the Accreditation Board for Engineering and Technology (ABET) and are related directly to an existing continuous quality improvement process implemented within the department. The faculty reviews student achievement on course objectives on a regular basis and using student data related to their understanding of the course learning objectives and performance on embedded indicators within graded course assignments.

5.1 Student perceptions of the camera project

Students completed a short, anonymous survey regarding their experiences with the camera project. Using a 7-point scale, student understanding, satisfaction, and improvement of technical communication skills were examined. Also, open-ended comments were obtained on the effectiveness of the experiment and methods to improve the camera project. For this pilot project, 11 completed surveys were analysed with a response rate of 31 %.

A majority of the respondents (73 %) indicated that they were satisfied with the variety of lab experiments (see Fig. 3). The mean score on satisfaction was 4.9, with 7 being very satisfied.

A majority (55 %) of students reported they were satisfied with the understanding of course material, while 45 % indicated no change.

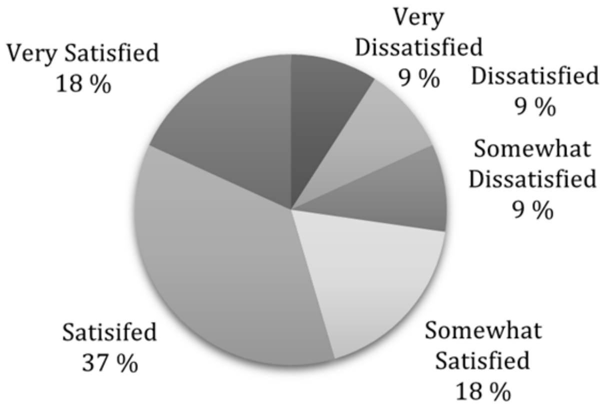

Fig. 3 Degree of satisfaction with the variety of laboratory experiments

When asked if their technical communication skills had improved as a result of the videos in lieu of a written report, 55 %, indicated a perceived improvement as shown in Fig. 4. In addition, a wide majority of the respondents (75 %) reported a perceived increase in their ability to share technical information through a medium other than written reports.

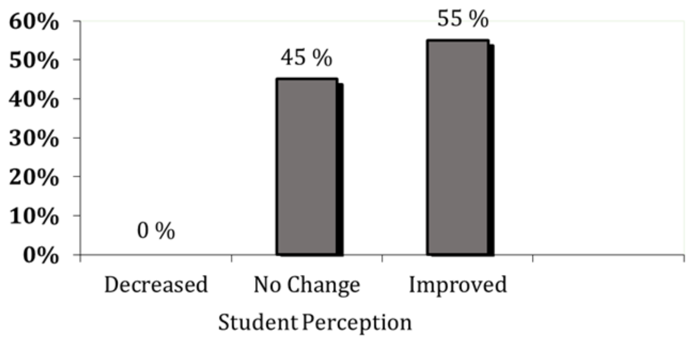

Fig. 4 Perception of technical communication skills after the experiment

Students offered the following comments during the assessment process.

- The cameras showed great resolution and helped with all of our projects
- When we had to turn in lab reports, I didn't prefer the videos. You won't necessarily do that in the future, whether it is in another class or in your job, and I would like to see the lab reports help prepare you for the future more or even better represent what you would be doing in future classes or your job. Other than that, I loved the lab!
- I loved them!
- They were great – more would improve the lab.
- The video quality wasn't as great as I had hoped for, but it got the job done.
- I enjoyed using them; however, there is a need to learn some form of digital editing software beforehand. Until some familiarity with the software was gained, the video reports were somewhat more time consuming. Using the footage to analyse failure tests, however, was quite useful in watching for fine detail.
- I enjoyed using them; however, there is a need to learn some form of digital editing software beforehand. Until some familiarity with the software was gained, the video reports were somewhat more time consuming. Using the footage to analyse failure tests, however, was quite useful in watching for fine detail.
- I would enjoy some hands-on experience with the GoPro cameras. I did enjoy the last couple of experiments where we were able to choose our own material, test, and present it. I also wish the GoPros were capable of better high-speed capture. The impact testing, in particular, was hard to document and analyse because of blurry shots.

5.2 Mechanical engineering faculty reviews

The Department of Mechanical Engineering faculty reviews course objectives and student performance as part of the continuous quality improvement process. Table 2 summarizes mean scores of faculty ratings before the cameras were introduced (spring 2012) and the following two years when cameras were used. A substantial improvement in learning objectives accomplished on treatment on metal alloys and a smaller improvement were recorded for the course objectives 2 and 3. This data is directly based on embedded indicators within graded assignments by taking the average over the entire class for that assignment/embedded indicator. The scale was A = 5, B = 4, C = 3, etc. with the average of these scaled grades taken over the entire class for the embedded indicators.

Table 2 Faculty ratings of course learning outcomes

Learning Objectives	Spring 2012	Spring 2013	Spring 2014
1. Analyse the effect of heat treatment on metal alloys.	3.7	4.5	4.7
2. Perform standard hardness, tensile, and impact tests on metals and polymers.	3.4	3.4	3.5
3. Present experimental results in laboratory reports.	3.4	3.5	3.5

As part of ABET continuous quality improvement, students rate their level of knowledge related to course objectives on a scale of 0 to 3. After the cameras were used, ratings were very high in the three learning objectives as shown in Table 3. Students had a high average score of 2.87 in in performing hardness, tensile, and impact tests. These mean score were quite encouraging and support other student perceptions and faculty reviews.

Table 3 Student perceptions of achievement from first semester of camera usage (scale is 0-3, n is 15)

Course Learning Objective	MIN	AVG	MAX	σ
Analyse the effect of heat treatment on metal alloys	1.0	2.47	3.0	0.64
Perform standard hardness, tensile, and impact tests on metals and polymer	2.0	2.87	3.0	0.35
Present experimental results in laboratory reports	2.0	2.67	3.0	0.49

6. Conclusion, limitations, and future research

6.1 Conclusion and discussion

Results from using the action camera and video productions are very encouraging regarding student learning and motivation. Students perceived their technical communication skills had increased as a result of the action camera experiment. Use of these cameras and associated video editing helped prepare these students for future coursework. Video reports are becoming an integral part of undergraduate courses, including the capstone Senior Design class for mechanical and electrical engineering majors.

Students seemed to be enthusiastic and asked permission to use the cameras for other classes where they needed to use the 120 fps video to determine how high an object bounced after being dropped from the walk through between buildings on campus. A graduate student also used the cameras to record the deformation of an aluminium honeycomb nosecone material during a simulated impact study. Also, these cameras seem ideal for other purposes, since they are all break-resistant, water-resistant, and student-resistant.

The use of the GoPro cameras in the materials science laboratory was a success, marred only by the first effort. Students indicated an improved understanding of material failure by visualizing the breakage and replaying the video. The video provided an opportunity to see a metal specimen undergo ductile or brittle failure over a span of seconds as opposed to the blink of an eye.

This technology may be used in other classes, such as business and technology, i.e. Operations Management. Likewise, while this innovative technique was used in a materials management class, the process may be expanded to other courses such as Entrepreneurship. For instance, a business plan may show a new product with only a picture, but students could implement this technique in their presentations. In addition, this video would bring the project to life and allow demonstration of the manufacturing process, testing, and being used by consumers. Presentations of strengths and features of many new ventures and products could be improved by using this technology.

6.2 Limitations and directions for future research

Since the research was designed to be exploratory in nature and thus was broad based in scope, only one laboratory experiment was conducted. The validity of the projects were measured by student perceptions, faculty ratings, and course evaluations. However, assessment of using cameras and video production should be measured in other classes with larger sample sizes.

Though the research provides interesting insights into student learning, limitations do exist. Although this innovation proposed in this study may have extended applications, the empirical tests rely on data collected from one mechanical engineering class. While no research has identified that this project in this class is fundamentally different, differences may exist in other classes. Future research would do well to integrate lessons learned in this experiment to other classroom settings and other disciplines. Specific examples are:

- *Computer Integrated Manufacturing* – Study the application of computer-aided design, computer-aided manufacturing, computer numeric control, robotics, programmable logic controllers and communication networks to achieve automated manufacturing.
- *Lean Production* – Explore applications of metal materials processing with an emphasis on lean manufacturing tools for reducing waste and streamlining production.
- *Advanced Manufacturing Processes* – Complete a survey of the latest manufacturing processes that are used in order to produce products that cannot be created with conventional manufacturing processes. Processes covered will include non-traditional machining methods, abrasive machining, advanced casting methods, specialized welding methods, and other high-end processes used in manufacturing industries.
- *Total Quality Management* – A study of the principles and practices of TQM to include leadership in quality, customer satisfaction, employee involvement, and continuous process improvement. Such TQM tools and techniques as quality function deployment and experimental design are studied.

Acknowledgement

The authors would like to thank the Department of Academic Transformation and Office of Academic Affairs, and the Office of Sponsored Research, The University of Texas at Tyler, for providing the grant money to purchase the GoPro Hero2 equipment.

References

[1] Goodhew, P.J., Bullough, T.J. (2006). Active learning in materials science and engineering, *Journal of Materials Education*, Vol. 28, No. 3-6, 161-169.

[2] Davies, C.H.J., Hines, P.J., Ringer, S.P. (2001). A flexible learning studio for materials science and engineering, In: *Towards Excellence in Engineering Education: Proceedings of the 12th Australasian Conference on Engineering Education*, *7th Australasian Women in Engineering Forum*, Brisbane, 245-250.

[3] Pinder-Grover, T., Green, K.R., Millunchick, J.M. (2011). The efficacy of screencasts to address the diverse academic needs of students in a large lecture course, *Advances in Engineering Education*, Vol. 2, No. 3, 1-28.

[4] Laoui, T., O'Donoghue, J. (2008). Development of a support environment for first year students taking materials science/engineering, *Research in Science & Technological Education*, Vol. 26, No. 1, 93-110, doi: 10.1080/02635140701847553.

[5] Kurt, A.O., Kubat, C., Öztemel, E. (2006). Web-based virtual testing and learning in material science and engineering, *International Journal of Engineering Education*, Vol. 22, No. 5, 986-992.

[6] Mikulski, M.A., Szkodny, T. (2011). Remote control and monitoring of AX-12 robotic arm based on windows communication foundation, In: Czachórski, T., Kozielski, S., Stańczyk, U. (eds.), *Man-Machine Interactions 2*, *Advances in Intelligent and Soft Computing*, Vol. 103, 77-83, Springer, Berlin, doi: 10.1007/978-3-642-23169-8_9.

[7] Avery, A., Jacob, J. (2013). Evaluation of motion capture techniques in microgravity, In: *51st AIAA Aerospace Sciences Meeting including the New Horizons Forum and Aerospace Exposition*, Dallas, Texas, USA, 10827-18240, doi: 10.2514/6.2013-731.
[8] Kindt, D. (2011). First impressions from recording in the classroom with a GoPro head-mounted camcorder, *Academic Journal of the School of Contemporary International Studies*, Vol. 11, 179-199.
[9] Tugrul, T.O. (2012). Student perceptions of an educational technology tool: Video recordings of project presentations, *Procedia – Social and Behavioral Sciences,* Vol. 64, 133-140, doi: 10.1016/j.sbspro.2012.11.016.
[10] Schultz, P.L., Quinn, A.S. (2013). Lights, camera, action! Learning about management with student-produced video assignments, *Journal of Management Education*, Vol. 38, No. 2, 234-258, doi: 10.1177/1052562913488371.
[11] Cochrane, T.A., O'Donoghue, M. (2008). Improving oral presentation skills of engineering students with the Virtual-i Presenter (ViP) program, In: *Proceedings of the 2008 AaeE Conference*, Yeppoon, Australia, 1-6.
[12] Armstrong, G.R., Tucker, J.M., Massad, V.J. (2009). Achieving learning goals with student-created podcasts, *Decision Sciences Journal of Innovative Education*, Vol. 7, No. 1, 149-154, doi: 10.1111/j.1540-4609.2008. 00209.x.
[13] Menekse, M., Stump, G.S., Krause, S., Chi, M.T.H. (2013). Differentiated overt learning activities for effective instruction in engineering classrooms, *The Research Journal for Engineering Education*, Vol. 102, No. 3, 346-374, doi: 10.1002/jee.20021.
[14] CNET Editors, GoPro Hero2 Outdoor Edition, from *http://reviews.cnet.com/digital-camcorders/gopro-hd-hero2-outdoor/4505-6500_7-35055132.html*, accessed August 14, 2013.
[15] McCaslin, S.E., Kesireddy, A., from YouTube Analytics: *http://www.youtube.com/user/UTTylerMEProfMc*, accessed February 15, 2013.
[16] Microsoft, Movie Maker – Microsoft Windows, *from http://windows.microsoft.com/en-us/windows-live/movie-maker*, accessed August 14, 2013.
[17] TechSmith, Camtasia Studio, from *http://www.techsmith.com/camtasia-2gslp.html?gclid=CI3ApNKf_bgCFdGj4AodPU4AFg*, accessed August 14, 2013.

APEM journal

Advances in Production Engineering & Management
Volume 10 | Number 2 | June 2015 | pp 97–107
http://dx.doi.org/10.14743/apem2015.2.195

ISSN 1854-6250
Journal home: apem-journal.org
Original scientific paper

Wear characteristics of heat-treated Hadfield austenitic manganese steel for engineering application

Agunsoye, J.O.[a,*], **Talabi, S.I.**[b], **Bello, O.**[a]

[a]Department of Metallurgical and Materials Engineering, University of Lagos, Akoka, Nigeria
[b]Department of Materials and Metallurgical Engineering, University of Ilorin, Ilorin, Nigeria

A B S T R A C T

The wear behaviour was investigated of heat treated Hadfield austenitic manganese steel (HAMnS). The wear test was carried out using spin on disc apparatus under different loading loads and speed conditions. A scanning electron microscopy (SEM), an X-ray diffractometer and micro-hardness testing machines were used for examining the morphology, compositions and to measure the hardness of the manganese steel, respectively. The results of the wear test showed that the sliding speed-time interactions effect gave the most significant effect on the austenitic manganese steel. The solution heat treatment programme increased the wear resistance of the alloy steel under increasing load, speed and time. The as-cast microstructure was characterized by heterogeneously dispersed chromium carbides second phase particle, and was responsible for the observed non-uniform wear rate. In regard to the solution heat treated HAMnS, the segregated carbides were dissolved at 1050 °C and uniformly dispersed within the matrix of its microstructure after rapid water quenching to room temperature. This later development was responsible for the uniform and improved wear resistance of the manganese steel casting. This work demonstrated significantly that there is a direct relationship between the second phase carbides, their distribution and the wear rate pattern of HAMnS casting.

A R T I C L E I N F O

Keywords:
Manganese steel
Wear behaviour
Solution heat treatment
Microstructure
Hardness

**Corresponding author:*
jagunsoye@unilag.edu.ng
(Agunsoye, J.O.)

Article history:
Received 18 November 2014
Revised 30 March 2015
Accepted 7 April 2015

1. Introduction

A lot of money has been spent on using electricity and explosive to break rocks. The motivation to reduce energy consumption has led to the use of non-explosive means to break rocks and extract valuable minerals [1]. The non-explosive means has advantage of avoiding sudden removal of plastic-elastic energy that can cause fracture by blasting. But due to wear, the materials used in breaking this rocks usually required early replacement. The replacement of item involves both material and manpower cost. There are different kinds of wear-resistant materials that are used for processing of solid mineral vis-a-vis crushing and grinding. The traditional materials include wear resistance high chromium iron, hyper-steel, medium carbon steel that are case-hardened, manganese steel etc. In general terms, the high chromium iron suitable for wear resisting applications fall within the compositional limits bounded by the austenitic phase field of the ternary liquidus surface of the iron, chromium, carbon diagram [2]. However the use of high chromium wear resistant iron comes at a huge cost. The material is also known to be characteristically very hard and brittle. Consequently this grade of material is prone to crack under repeated impact load in areas where impact is common [3]. They are usually used in the quarry as cast plate for bottom liners and as side plate for crushing of hard solid minerals. Regrettably once they are broken, there is no possibility of salvage through hard-facing with wear resistance electrodes. Because of the frequent breakage of high chromium resistant iron, there is a need for the development of a wear-resistant alloy steel that will have high wear resistant, tough and hard at the same time. So in 1882, austenitic manganese rich steel (Hadfield steel), containing between 11 % and 14 % manganese and about 1.2 % carbon, was developed about 13 decades ago and its consequent use for high-wear applications [4]. Major advantages of this material include its toughness and ductility, and the fact that continuous surface impacts result in work-hardening without any increase in brittleness. Consequently, Hadfield steels and their technological descendants provide both strength and abrasion resistance; qualities that are essential for wear parts that can withstand the rigors of the crushing process [5]. It has also the requisite toughness to undergo plastic deformation without cracking. Presently, the major challenge facing the quarrying industry in Nigeria is the high cost associated with worn-out wear plate that are predominantly made or manufactured from manganese steel.

Researchers have performed many studies to improve the wear resistance of Hadfield steels [6-9]. Microstructural phase transformation which is temperature dependent can be employed as a route for enhancing the wear characteristics of Hadfield austenitic manganese steel through the interplay of heat treatment. In the heat treatment process, the grain size in austenitic manganese steels before quenching is tremendously influenced by diffusive and diffusionless phase transformations, and precipitation [10]. The austenite grain size affects overall mechanical properties such as strength, hardness and ductility, hence its wear behaviour. Therefore, the influence of, solution heat treatment on the wear resistance of a typical Hadfield austenitic manganese use in quarrying industry was investigated.

2. Materials and methods

2.1 Material preparation

A sample representative from Hadfield austenitic manganese steel with composition of equivalent specification to NFMn128C was taken from a batch of 500 kg electric induction furnace melt to cast 4 bar of 200 × 11 × 11 mm to conduct the experiment. The charged materials used consist of 203 kg foundry returns, 220 kg low carbon steel, 10 kg of low carbon Ferro manganese, 65 kg high carbon Ferro manganese, 8 kg low carbon Ferrochromium, 2.19 kg Ferro silicon and 2.24 kg graphite powder respectively. The melting was carried out in a neutral lined refractory furnace. A digital pyrometer with disposable thermocouple tip was used for temperature measurement during melting and pouring. The molten metal was poured into an improvised CO_2 moulds in a mechanized foundry situated in Sango-Otta at the outskirt of Lagos, Nigeria.

2.2 Method

Patterns of dimension 202 × 11.2 × 11.2 mm were produced for the sand casting of the experiment. The sand used for the moulds was prepared by mixing dried silica sand, sodium silicate, water and bentonite in compliance to British standard. Thereafter, CO_2 gas was passed through the moulds for 80 seconds to cure the mould sand. To ensure correct mould identification, the moulds were labelled as A, B, C and D respectively. The charge make-up for the melt consist of Mn-Steel foundry returns (1.1 % C, 0.64 % Si, 12.4 % Mn, 1.2 % Cr, 0.006 % S, 0.005 % P, and 84.65 % Fe), Steel (0.20 % C, 0.35 % Si, 0.42 % Mn, 0.005 % S, 0.005 % P, and 99.02 % Fe), Low Carbon Ferro Manganese (0.23 % C, 75 % Mn), High Carbon Ferro Manganese (1.1 % C, 62 % Mn), Medium Carbon Ferro Chromium (0.5 % C, 67 % Cr), Ferro Silicon (0.02 % C, 70 % Si) and Graphite Powder (67 %).

The estimated charge make was calculated from Eq. 1.

$$\%(M) = \frac{(FeA/S)\%}{F_c} Q \tag{1}$$

In Eq. 1, M denotes melt, FeA denotes ferroalloy, S denotes scrap and F_c denotes furnace capacity. The furnace capacity represents the total charge in (kg), the Q represents the quantity of charge and % melt represent elemental concentration in the melt.

The standard compositions containing the lower and upper ranges of the specification for the melt of equivalent standard to NFMN128C is presented in Table 1.

Manganese as an element exhibits high oxidation tendency, therefore the manganese composition was deliberately calculated to be higher than the upper limit to ensure that the percentage of manganese is within the limit as a result of expected oxidation during holding of the molten metal in the furnace and de-slagging.

The raw materials as contained in the charge make-up in Table 2 for the melt were charged into the furnace in a particular order. The low carbon steel was charged first into a 500 kg medium frequency electric furnace lined with a neutral refractory material and allowed to melt completely. The selection of a neutral refractory was made deliberately to minimize furnace wall erosion as a result of slag attack. This was followed by the charging of the foundry returns, Ferro silicon, High carbon and Low carbon Ferro manganese and lastly graphite powder. The melting was completed after 94 minutes. The temperature of the molten bath was taken by a digital probe pyrometer with a disposable tip and recorded on an improvised daily furnace report. All procedures including personnel safety were observed during the melting and pouring operation.

The actual composition obtained after melting is presented in Table 3. The molten metal was poured at 1410 °C into the improvised CO_2 moulds, and allowed to solidify to room temperature after 12 h before they were knocked out and shot blasted. The 4-number castings were carefully fettled on a table grinding machine to the required dimensions 200 × 10 × 10 mm. During the grinding, care was taken to avoid work hardening on the surface of the casting.

Table 1 Chemical analysis result of melt of equivalent standard to NFMN128C

Specification	Elemental composition (%)					
	C	Si	Mn	Cr	S	P
Upper limit	1.30	0.80	14.00	1.50	0.005	0.005
Lower limit	1.00	0.60	12.00	1.00	0.005	0.005
Aim	1.28	0.70	14.34	1.52	0.004	0.005

Table 2 The Estimated charge make-up for Hadfield austenitic manganese steel

Description	Charge (kg)	Elemental composition (%)						
		C	Si	Mn	Cr	S	P	Fe
Foundry returns	203	0.437	0.25	4.84	0.47	0.002	0.002	bal
Steel	220	0.085	0.15	0.18	-	0.002	0.002	bal
Low Carbon Fe-Mn	10	0.004	-	1.46	-	-	-	-
High Carbon Fe-Mn	65	0.139	-	7.87	-	-	-	-
Ferro Chromium	8	0.007	-	-	1.05			-
Ferro Silicon	2.19	0.000	0.30	-	-	-	-	-
Graphite	2.24	0.555	-	-	-	-	-	-
Total	512	1.278	0.70	14.34	1.52	0.004	0.005	bal

Table 3 The compositional results obtained from bench top arc spectrometer

Elemental composition (%)					
C	Si	Mn	Cr	S	P
1.29	0.68	13.72	1.49	0.005	0.005

2.3 Heat treatment

The solution heat treatment process involves heating the sample at a particular heating rate. The choice of the heating rate depends on some factors such as the composition of the sample, shape of casting and the section thickness among other. For low carbon alloys and other alloy like manganese steels, their propensity to crack is extremely low, as such, the heating rate of 75 °C per hour. For high carbon specification or casting where warping of the sample may occur, a lower heating is adopted. The sample was heated to 1050 °C and held at this temperature for 24 min to allow the segregated carbides dissolve completely in solution in accordance to British standard. There after it was quenched quickly in a 500 l agitated water tank and allowed to cool room temperature.

2.4 Microstructural determination

A sample representative was taken from one as-cast and one heat treated cast bar. The surfaces were carefully prepared grinding on a tehrapol-31 machine, then polished with Allegrol with diamond suspension using a colloidal suspension of 0.04 μm silicon dioxide before they are etched in a solution of 100 ml alcohol and 3 ml HNO_3 acid at the Metallographic laboratory, Department of Mechanical Engineering. University of Ottawa, Ontario, Canada. An optical inverted Metallurgical microscope was used to study the microstructures. On the other hand, the morphology of the as-cast and heat treated samples were carried out using Scanning Electron Microscope (SEM) and Energy Dispersive Spectrum (EDS). The surface morphology of the worn out sample was also examined.

2.5 Micro-hardness value determination

Sample representatives were cut from the as-cast and heat treated bars for hardness testing. The samples were casted into resin mould, ground flat and polished. The hardness test was carried out on a Duramin-1 micro-hardness tester struers. An average of five measurements of hardness values was taken for as cast and heat treated manganese steel.

2.6 Wear test

Abrasive wear test were carried out on two prepared manganese steel castings (as-cast and heat treated) samples using pin-on-disc type equipment [11]. The wear test was carried out under varied load, and speed. After test each cycle of wear test, the mass of the worn out samples was measured with the aid of a digital weighing device with 0.001 mg accuracy to obtain the weight lost. Weight lost from the tests was used to calculate specific wear rate W, a parameter which defines wear severity from Eq. 1. From Eq. 1, V denotes volume loss of worn out sample, d_s denotes sliding distance, and L denotes applied load.

$$W = \frac{V}{d_s L} \tag{2}$$

The surface morphology of the worn out sample after the wear test was examined using optical microscope. The examined microstructure of the worn out, heat treated sample under high speed 4.72 m/s and 16 kN load is presented in Fig. 10. The surface morphology is characterized by needle like martensitic structure.

3. Results and discussion

3.1 Hardness and XRD test results

The result of the hardness test is presented in Table 4.

The indentation photo taken during the micro-hardness test is shown in Fig. 1(a) and Fig. 1(b) for heat treated and as-cast samples respectively. The solution heat treatment process inrease the hardness of the HAMnS sample. The increase in hardness might be due to fairly uniform distribution of the carbide phase in the austenite phase [2].

Table 4 Results of micro-hardness measurement

Description	Hardness, (HB)
As-cast Mn-steel	188
Heat treated Mn-steel	220

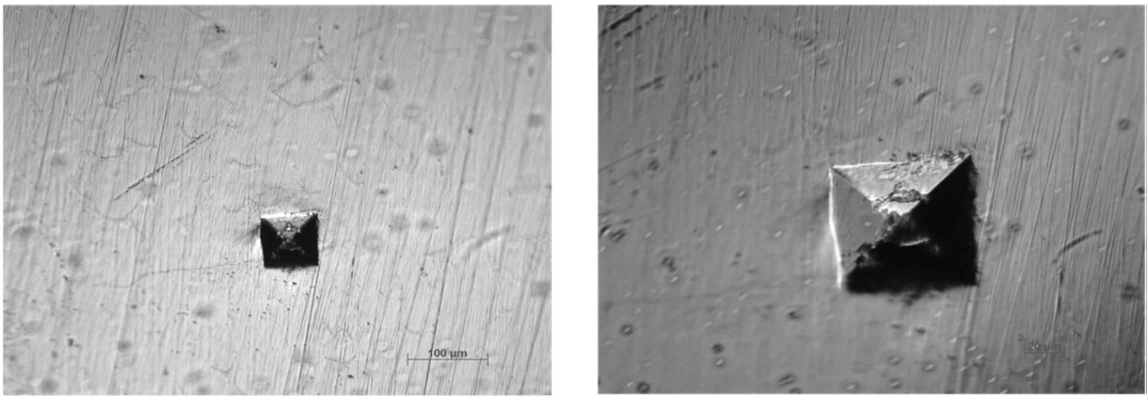

(a) (b)

Fig. 1 (a) Heat treated HAMnS indentation; (b) As-cast HAMnS indentation

The identified phases and compound formula from the XRD test for the manganese steel casting is presented in Table 5.

Table 5 Identified phases and their chemical formula

Score	Compound name	Chemical formula
38	Manganese	Mn
23	Carbon	C
21	Iron	Fe
21	Iron Silicon Carbide	$Fe_9\ Si\ C_{0.4}$
14	Manganese Silicon Carbide	$Mn_{22.6}\ Si_{5.4}\ C_4$
12	Chromium Carbide	$Cr_4\ C_{1.06}$
17	Manganese Silicon	Mn Si

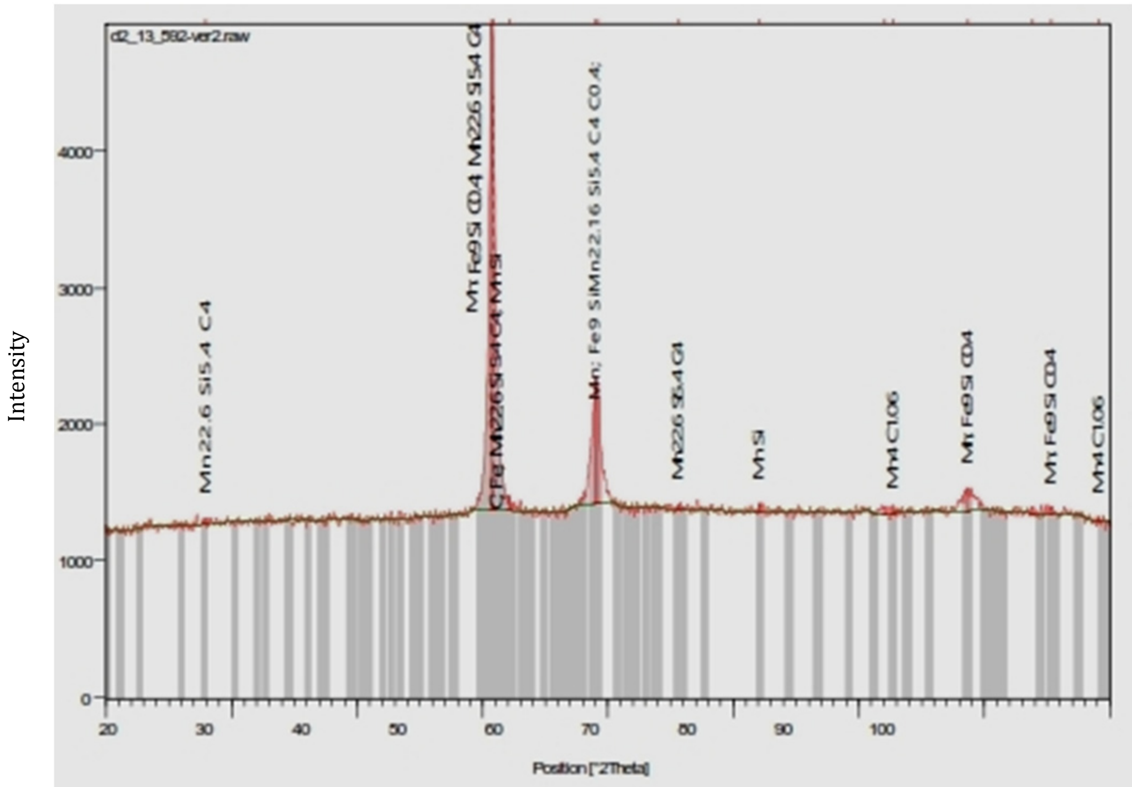

Fig. 2 The XRD profile of elemental segregation of manganese steel

3.2 Comparism between wear results and microstructure of as-cast manganese steel

Fig. 3 represents a graphical behaviour of the wear test results obtained for different load at the speed of 2.36 m/s for as-cast HAMnS. There is a general decrease in wear rate with increase in load. These phenomena may be attributable to increase interlocking of dislocation movement and to some extend work- hardening characteristics of the alloy. This same observed behaviour is replicated in a similar, but in a more pronounced manner at higher speed 4.72 m/s (Fig. 6). Hence, it can be infer that speed has significant effect on the wear behaviour of the manganese steel sample.

The observed non-uniformity in the wear profile curves of Fig. 1 and Fig. 2 can be attributed to the in-homogeneity of the as-cast HAMnS as revealed by the microstructure see Fig. 3. A non-uniform dispersion of the second phase (inter-metallic carbide) in the microstructure can be observed. The more heterogeneous the distribution of second phase particles, the more irregular the wear pattern of the as-cast HAMnS. This revealed that there is a strong relationship between distribution of second phase (Chromium carbide) and the wear nature of manganese steel.

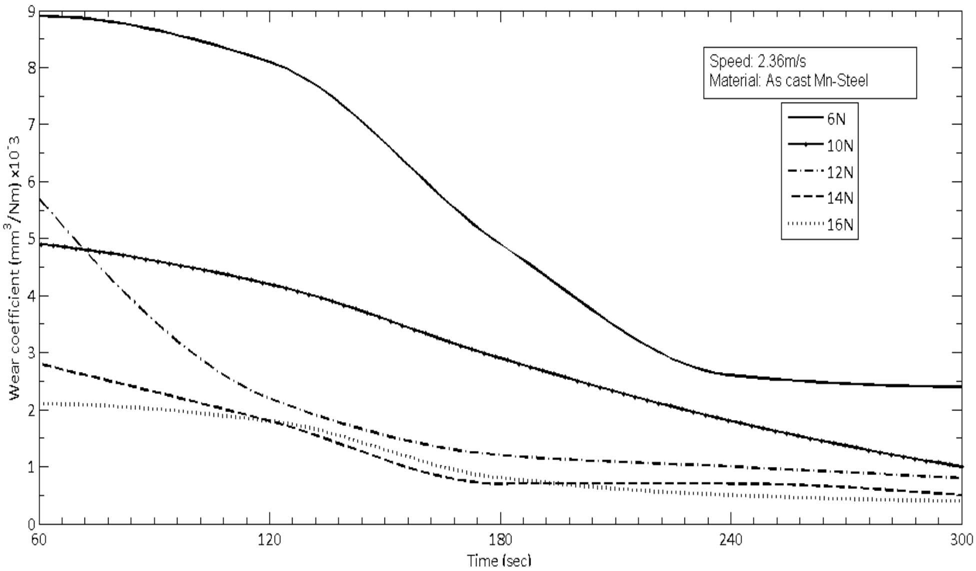

Fig. 3 Wear rate of as-cast HAMnS with time at 2.36 m/s and varying loads

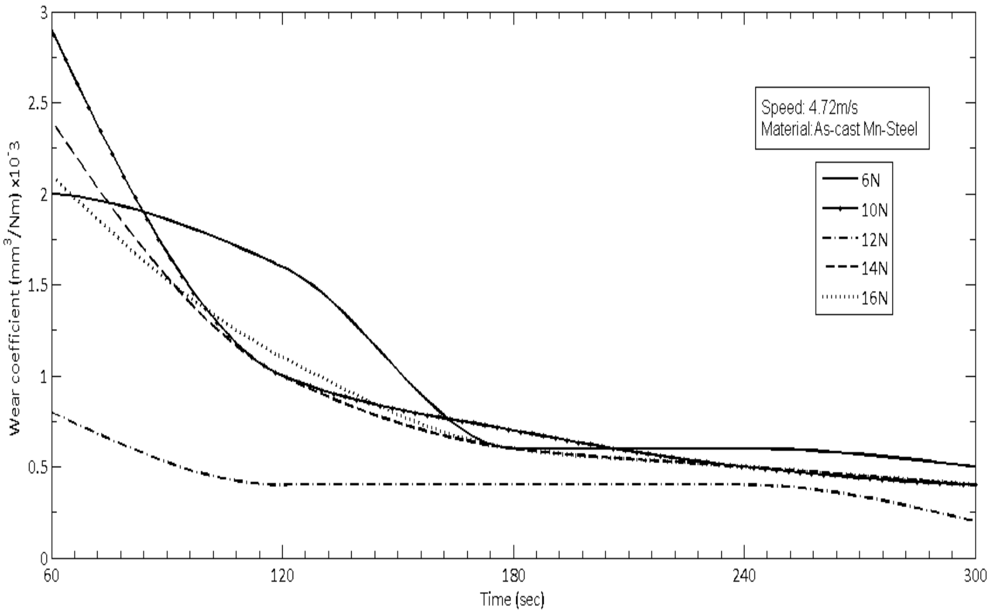

Fig. 4 Wear coefficient of as-cast HAMnS with time at 4.72 m/s for varying load

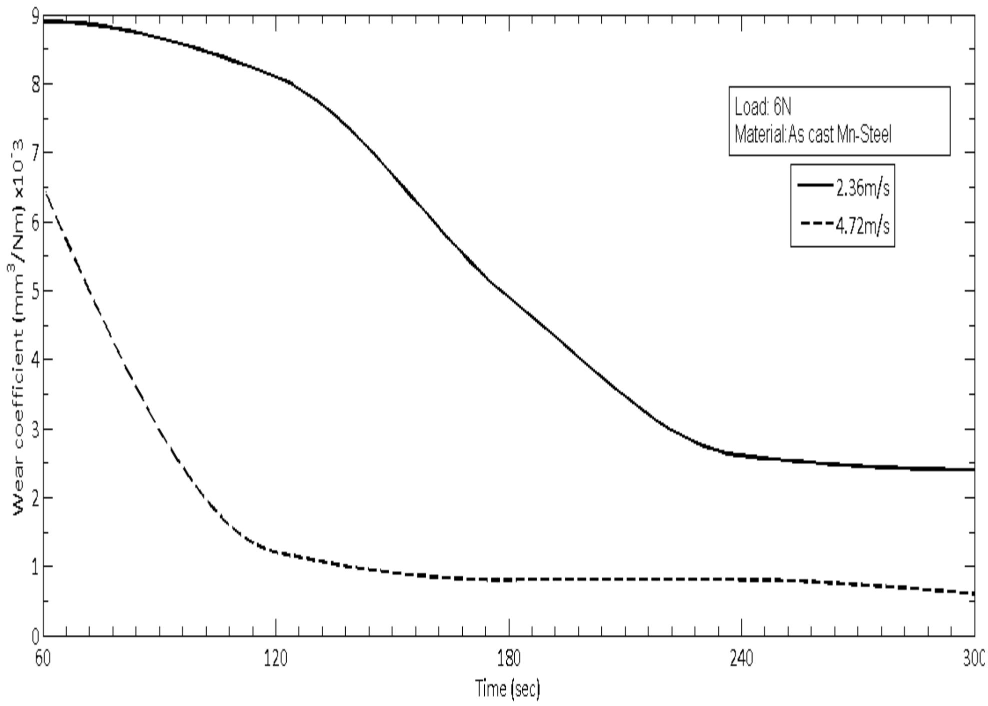

Fig. 5 Wear rate of As-cast HAMnS with time at 2.36 m/s and 4.72 m/s for load 6N

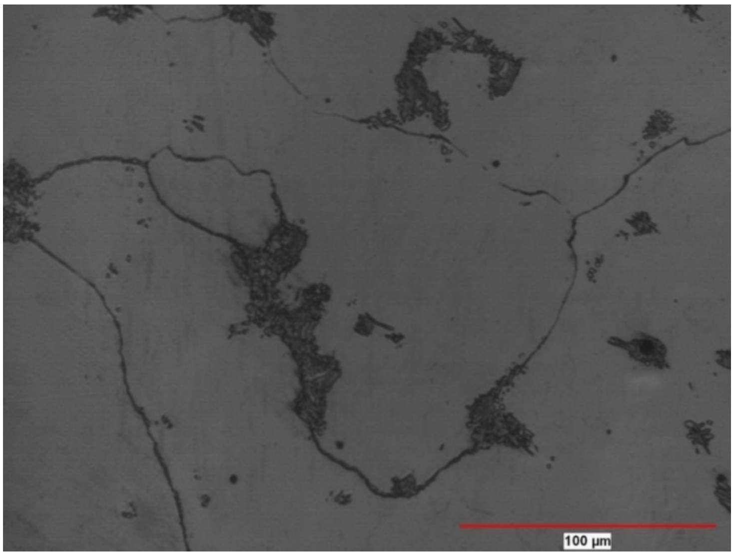

Fig. 6 The Optical micrograph of as-cast manganese steel showing significant heterogeneously dispersed chromium carbide within the austenite matrix of the microstructure at 100x

The wear rate of the HAMnS reduces significantly as the speed increases (Fig. 5). This further justifies the earlier assumption that speed has significant on the wear rate of the HAMnS sample. Increasing speed tends to improve the wear behaviour of the Mn-steel sample.

3.3 Comparison between wear results and microstructure of heat treated manganese steel

Fig. 7 shows smoother wear profile compared to Fig. 3. This can be attributed to the homogeneity of the heat treated manganese steel as revealed in the microstructure obtained after heat treatment (Fig. 9). The second phase particle (chromium carbide) as shown in Table 5 and Fig. 2 in the Xray-Diffraction result is uniformly dispersed with the austenite matrix. This development was attained after heat treatment (hardening) operation was carried out when the heterogeneously segregated second phase chromium carbide (Cr4C1.06) particle were dissolved in solution at 1050 °C, and quench in agitated water to trap the carbide within the matrix of the austenite.

A marked effect of load which became almost constant with increasing can also be observed. Time has no significant effect on the wear rate of Mn-steel sample. Similar to the as-cast sample, Fig. 8 shows that speed has significant effect on the wear behaviour of the heat treated sample.

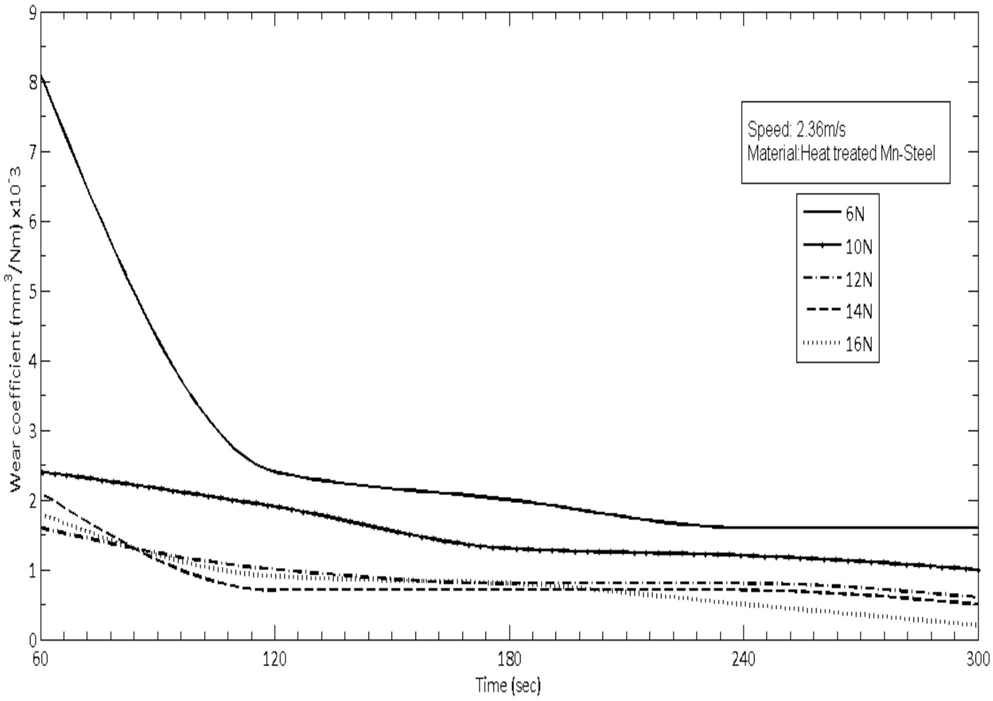

Fig. 7 Wear rate of Heat treated Mn-Steel with time at 2.36 m/s for varying load

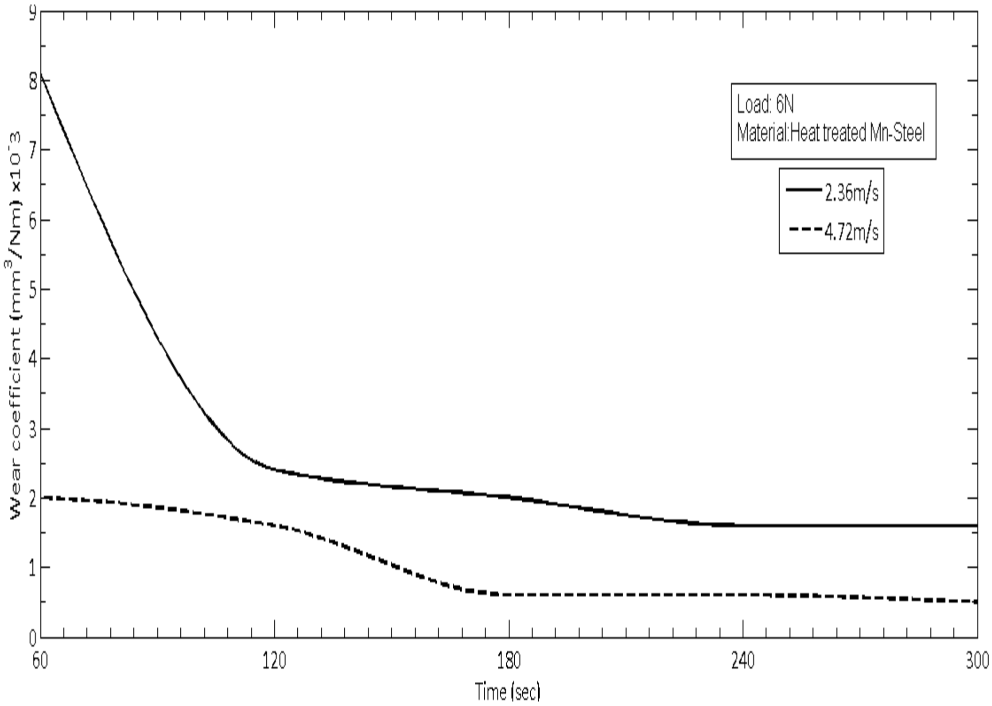

Fig. 8 Wear rate of Heat treated Mn-Steel with time at 2.36 m/s and 4.72 m/s, load 6N

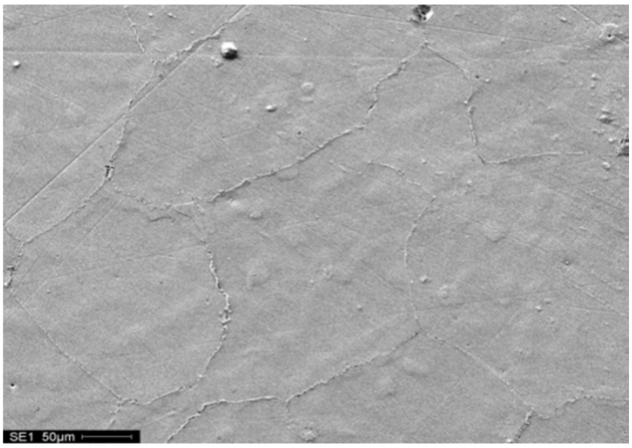

Fig. 9 The Optical micrograph (100x) of heat-treated manganese steel showing highly homogenous structure

The examined microstructure of the worn out, heat treated sample under high speed 4.72 m/s and 16 kN load is presented in Fig. 10. The surface morphology is characterized by needle like martensitic structure.

Fig. 10 Optical micrograph at 100x magnification of heat-treated manganese steel worn out- surface with evidence of high work hardenability after wear test

Fig. 11 shows the result of SEM and EDS analysis of the as-cast HAMnS. It was observed from Fig. 11 that the SEM micrograph is heterogamous in nature. This observation is similar to the Optical microstructure obtained in Fig. 6. The corresponding EDS corroborate the high degree of carbide segregation of iron and manganese.

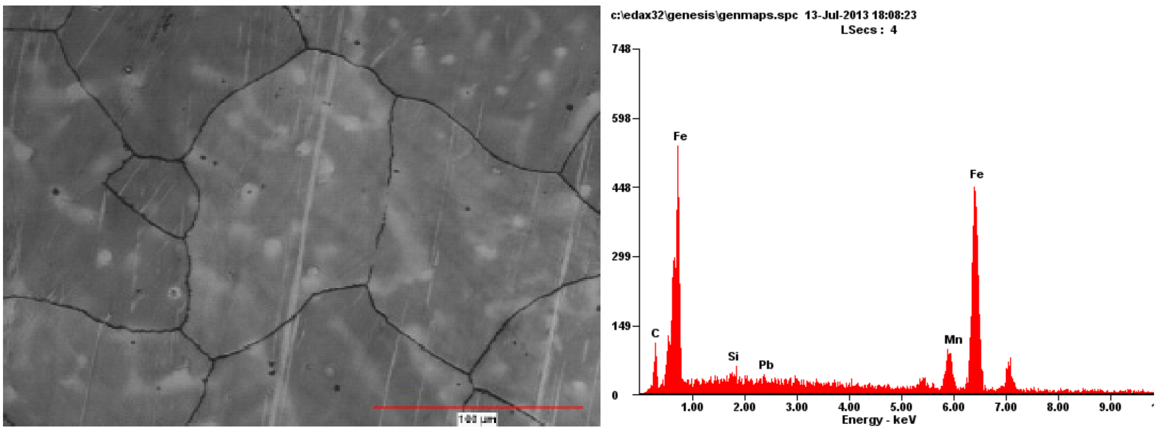

Fig. 11 The SEM micrograph and EDS of As-cast manganese steel

The SEM micrograph with the corresponding EDS of the heat treated manganese steel is shown in Fig. 12. It was observed from the micrograph that the second phase chromium carbide particle is uniformly dispersed with the austenitic matrix. Again, this observation collaborated the earlier results obtained in Fig. 9 and agreed with the result of [5]. The degree of carbide segregation had been reduced considerably from the corresponding energy dispersion spectrum for heat treated HAMnS.

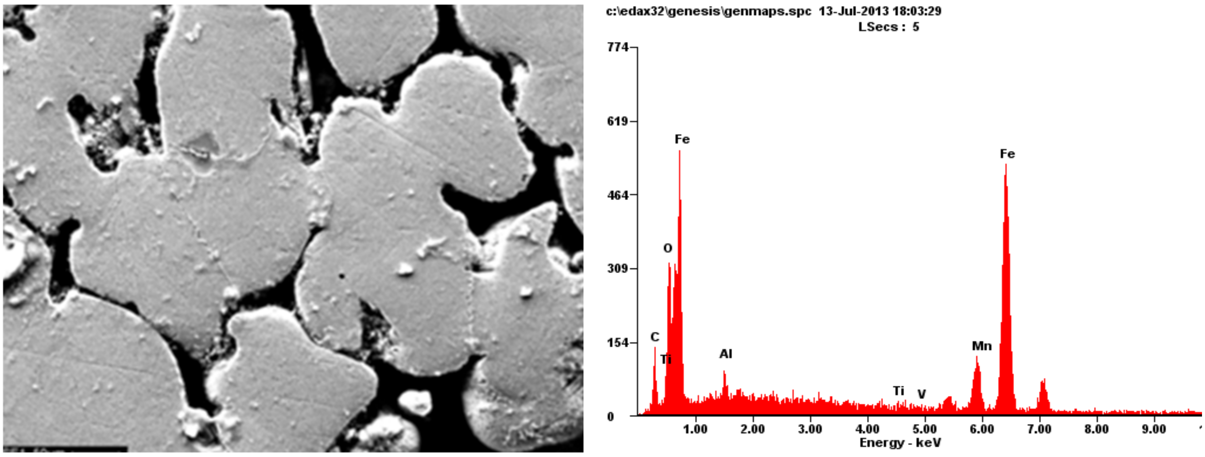

Fig. 12 The SEM and EDS micrograph of heat treated manganese steel

4. Conclusion

The wear behaviour of heat treated Hadfield austenitic manganese steel has been investigated. From the results of the investigations on the heat treated HAMnS the following conclusion were drawn.

1. The morphology and size of carbide phase has significant effect on the wear resistance of austenitic manganese steel.
2. The sliding speed-time interactions effect gave the most significant effect on the austenitic manganese steel
3. The solution heat treatment programme increased the wear resistance of the alloy steel under increasing load, speed and time.
4. The improved wear resistance of the manganese steel obtained was due to the formation of hard carbide phase within the matrix structure of austenitic manganese steel.
5. The wear behaviour of austenitic manganese steel can considerably be optimized by solution heat treatment and adequate quenching to redistribute the heterogeneous and segregated second phase chromium carbide to form a more homogenous and uniformly dispersed second-phase particle to enhance the wear resistance of the manganese steel.

Acknowledgement

The authors acknowledge the support from Nigerian Foundries Limited, Ilupeju Industrial Estate, Lagos for the exclusive use of her facilities to carry out this study. The authors would like to thank Dr. Micheal Nganbe, an associate Professor at the Department of Mechanical Engineering, University of Ottawa, Ontario Canada for his technical input and Dr. Mohammed Yadouzi a research fellow at the same Department who facilitated optical micrographs tests and interpretations.

References

[1] Mokken, A.H. (1969). The use of stainless steels in the mining industry; In: *Proceedings Symposium on Stainless steels*, Johannesburg, 83-102.

[2] Agunsoye, J.O., Talabi, S.I., Abiona, A.A. (2013). On the comparison of microstructure characteristics and mechanical properties of high chromium white iron with the hadfield austenitic manganese steel, *Journal of Minerals and Materials Characterization and Engineering*, Vol. 1, 24-28, doi: 10.4236/jmmce.2013.11005.

[3] Studnicki, A., Kilarski, J., Przybył, M., Suchoń, J., Bartocha, D. (2006). Wear resistance of chromium cast iron – research and application, *Journal of Achievements in Materials and Manufacturing Engineering*, Vol. 16, No. 1-2, 63-73.

[4] Agunsoye, J. (2009). *The Wear Characteristics of Austenitic Manganese Steel Casting*, PhD Thesis, University of Lagos, Nigeria.

[5] Balogun, S.A., Esezobor, D.E., Agunsoye, J.O. (2008). Effect of melting temperature on the wear characteristics of austenitic manganese steel, *Journal of Minerals and Materials Characterization and Engineering*, Vol. 7, No. 3, 277-289.

[6] Yan, W., Fang, L., Sun, K., Xu, Y. (2007). Effect of surface work hardening on wear behavior of Hadfield steel, *Materials Science and Engineering: A*, Vol. 460-461, 542-549, doi: 10.1016/j.msea.2007.02.094.

[7] Abbasi, M., Kheirandish, S., Kharrazi, Y., Hejazi, J. (2010). On the comparison of the abrasive wear behavior of aluminum alloyed and standard Hadfield steels, *Wear*, Vol. 268, No. 1-2, 202-207, doi: 10.1016/j.wear.2009.07.010.

[8] Bouaziz, O., Allain, S., Scott, C.P., Cugy, P., Barbier, D. (2011). High manganese austenitic twinning induced plasticity steels: A review of the microstructure properties relationships, *Current Opinion in Solid State and Materials Science*, Vol. 15, No. 4, 141-168, doi: 10.1016/j.cossms.2011.04.002.

[9] Aribo, S., Alaneme, K.K., Folorunso, D.O., Aramide, F.O. (2010). Effect of precipitation hardening on hardness and microstructure of austenitic manganese steel, *Journal of Minerals and Materials Characterization and Engineering*, Vol. 9, No. 2, 157-164.

[10] Xu, Y., Chen, Y., Xiong, J., Zhu, J. (2001). Mechanism of strain-induced nanocrystallization of Hadfield steel under high energy impact load, *Acta Metallurgica Sinica*, Vol. 37, 165-70.

[11] Agunsoye, J.O, Ochulor, E.F., Talabi, S.I., Olatunji, S. (2012). Effect of manganese additions and wear parameter on the tribological behaviour of NFGrey (8) cast iron, *Tribology in Industry*, Vol. 34, No. 4, 239-246.

Calendar of events

- European Symposium on Intelligent Materials 2015, Kiel, Germany, June 10-12, 2015.
- ICIT 2015: International Conference on Industrial Technology, Vienna, Austria, June 21-22, 2015.
- 10th International Conference on Additive Manufacturing & 3D Printing, Nottingham, UK, July 7-9, 2015.
- AIM – 2015 IEEE International Conference on Advanced Intelligent Mechatronics, Busan, South Korea, July 7-11, 2015.
- 27th European Conference on Operational Research, Glasgow, UK, July 12-15, 2015.
- ICME 2015: International Conference on Manufacturing Engineering, Stockholm, Sweden, July 13-14, 2015.
- 17th International Conference on Industrial and Intelligent Information Engineering, Oslo, Norway, July 17-18, 2015.
- The 5th International Conference on Simulation and Modeling Methodologies, Technologies and Applications, Colmar, France, July 21-23, 2015.
- Additve Manufacturing + 3D Printing Conference & Expo, Boston, United States, August 2-5, 2015.
- 17th International Conference on Internet Manufacturing and Services, Amsterdam, The Netherlands, August 6-7, 2015.
- 17th International Conference on Modelling, Optimization and Simulation, Venice, Italy, August 13-14, 2015.
- XXIV International Materials Research Congress, Cancon, Mexico, August 16-20, 2015.
- 17th International Conference on Emerging Trends in Engineering and Technology, Geneva, Switzerland, September 7-8, 2015.
- IEEE 20th Conference on Emerging Technologies & Factory Automation, Luxembourg, Luxembourg, September 8-11, 2015.
- ICMSE 2015: International Conference on Manufacturing Science and Engineering, Berlin, Germany, September 14-15, 2015.
- 23rd International Conference on Materials and Technology, Portorož, Slovenia, September 27-30, 2015.
- IEEE/RSJ International Conference on Intelligent Robots and Systems (IROS 2015), Hamburg, Germany, September 28 – October 2, 2015.
- 26th DAAAM International Symposium 2015, Zadar, Croatia, October 21-24, 2015.
- 17th International Conference on Engineering Systems Modeling, Simulation and Analysis, Paris, France, October 29-30, 2015.
- ASME – International Mechanical Engineering Congress & Exposition (IMECE), Houston, Texas, United States, November 13-19, 2015.
- 17th International Conference on Supply Chain and Logistics Management, Dubai, UAE, November 24-25, 2015.
- 17th International Conference on Automotive Engineering and Intelligent Manufacturing, Bangkok, Thailand, December 17-18, 2015.

Notes for contributors

General

Articles submitted to the *APEM journal* should be original and unpublished contributions and should not be under consideration for any other publication at the same time. Extended versions of articles presented at conferences may also be submitted for possible publication. Manuscript should be written in English. Responsibility for the contents of the paper rests upon the authors and not upon the editors or the publisher. Authors of submitted papers automatically accept a copyright transfer to *Production Engineering Institute*, *University of Maribor*.

Submission of papers

A submission must include the corresponding author's complete name, affiliation, address, phone and fax numbers, and e-mail address. All papers for consideration by *Advances in Production Engineering & Management* should be submitted by e-mail to the journal Editor-in-Chief:

Miran Brezocnik, Editor-in-Chief
UNIVERSITY OF MARIBOR
Faculty of Mechanical Engineering
Production Engineering Institute
Smetanova ulica 17, SI – 2000 Maribor
Slovenia, European Union
E-mail: editor@apem-journal.org

Manuscript preparation

Manuscript should be prepared in *Microsoft Word 2007* (or higher version) word processor. *Word .docx* format is required. Papers on A4 format, single-spaced, typed in one column, using body text font size of 11 pt, should have between 8 and 12 pages, including abstract, keywords, body text, figures, tables, acknowledgements (if any), references, and appendices (if any). The title of the paper, authors' names, affiliations and headings of the body text should be in *Calibri* font. Body text, figures and tables captions have to be written in *Cambria* font. Mathematical equations and expressions must be set in *Microsoft Word Equation Editor* and written in *Cambria Math* font. For detail instructions on manuscript preparation please see instruction for authors in the *APEM journal* homepage *apem-journal.org*.

The review process

Every manuscript submitted for possible publication in the *APEM journal* is first briefly reviewed by the editor for general suitability for the journal. Notification of successful submission is sent. After initial screening the manuscript is passed on to at least two referees. A double-blind peer review process ensures the content's validity and relevance. Optionally, authors are invited to suggest up to three well-respected experts in the field discussed in the article who might act as reviewers. The review process can take up to eight weeks. Based on the comments of the referees, the editor will take a decision about the paper. The following decisions can be made: accepting the paper, reconsidering the paper after changes, or rejecting the paper. Accepted papers may not be offered elsewhere for publication. The editor may, in some circumstances, vary this process at his discretion.

Proofs

Proofs will be sent to the corresponding author and should be returned within 3 days of receipt. Corrections should be restricted to typesetting errors and minor changes.

Offprints

An e-offprint, i.e., a PDF version of the published article, will be sent by e-mail to the corresponding author. Additionally, one complete copy of the journal will be sent free of charge to the corresponding author of the published article.

APEM *journal*

Advances in Production Engineering & Management

Production Engineering Institute (PEI)
University of Maribor
APEM homepage: apem-journal.org

Volume 10 | Number 2 | June 2015 | pp 55-110

Contents

ISSN 1854-6250
9 771854 625008

apem-journal.org